Modeling ore generation in a magmatic context

Jean-Louis Vigneresse, Laurent Truche

Version of Record: https://www.sciencedirect.com/science/article/pii/S0169136819301519
Manuscript_b9802844f18bcdd9de53d3b23f96819e

Modeling ore generation in a magmatic context

Jean-Louis Vigneresse*[1], Laurent Truche[2]

[1] GéoRessources, UMR 7539, Université de Lorraine, 54506 Vandoeuvre/Nancy Cédex, France jean-louis.vigneresse@univ-lorraine.fr

[2] ISTerre, Université de Grenoble-Alpes, 38400 Saint-Martin-d'Hères, France. laurent.truche@univ-grenoble-alpes.fr

Abstract

Magmatic ore deposit models are constructed from a set of measurables (e.g., ore grade, fluid composition, structure) from which important parameters (temperature, pressure, chemistry) can be estimated and possible genetic processes can be constrained. Such models include direct, inverse or iterative problems. Direct problems separately consider an Eulerian and a Lagrangian formulation. In the first case, an analytical approach describes the bulk system from an external frame, whereas the Lagrangian approach provides a description from a discrete element attached to the system. Conversely, inverse problems mostly rely on a system of equations or differential equations. Their solution requires a matrix inversion, using statistical criteria to bracket errors. Subsequently, an iterative approach is adopted, commencing with an initial bulk model that is successively refined to fit the observations. The direct problem always results in a unique solution, though the formulation is highly overdetermined. Such unique solution highly depends on the input parameters, and multiple solutions vary with the initial imposed conditions. Conversely, the inverse problem is

underdetermined by construction (Atlan, 2001). Accordingly, it provides a set of solutions, generally identified and separated by statistical tests,as exemplified bythe least squares approximation. Both methods intrinsically ignore feedback loops. Iterative methods are weak in quantifying the results. Based on the insights gained from this review, we developed a new integrative model for porphyry deposits that relies on the magmatic segregation of metals through a fluid sparging process. A formulation under the direct problem basically considers the enrichment factor for groups of metals (e.g., Cu, Mo, Au). A Lagrangian approach using a lattice Boltzmann model examines metal diffusion from the melt toward an immiscible phase, commonly a salty aqueous fluid. Metals first diffuse in the melt, the motion of which slows down when the mush development reduces the porosity, thus tapping the mobile fluid phase. Gas bubbles turn to tubes. They offer more mobility and allow the progression of the fluid phase, leading to metal advection, followed by metal precipitation. The quantitative results are poorly constrained owing to the large uncertainties on the input parameters but the metal enrichment factor fits observations from crustal abundance to ore grade levels. Nevertheless, the results aid in designing an inverse approach linking metal enrichment to metal partitioning, diffusion and viscous melt motion. From this approach, a simple diagram can be deduced using a logarithmic scale to smooth the parametric uncertainties. The diagram serves to illustrate the link between the above parameters and metal enrichment, also explaining differences in ore grade for different metals-magma pairs.

Keywords: ore formation; diffusion/advection; direct and inverse problem; iterative process; porphyry deposits

Number pages 58 lines 14310 characters 110600 Figures 11

submitted to Ore Geology Reviews as OREGEO_2019_137_R4

Version 4/27/20

*Corresponding author Jean-Louis Vigneresse

GéoRessources BP 70239 54506 Vandoeuvre/Nancy Cedex France

tel 00 333 83 20 47 68 fax 00 333 83 68 47 01

email jean-louis.vigneresse@univ-lorraine.fr

Declaration of interest

The present authors worked equivalently on the paper. JLV built the model. Many inputs to the text and figures, as well as encouragements, were provided by colleagues (LT) and Antonin Richard. They declare not having any commercial or associative interest that could represent conflicts of interest in connection with the present work.

1. Introduction

Magmatic ore deposits are spatially and genetically associated with igneous rocks enriched, often up to percent levels, in base and precious metals such as Cu, Ag, Au, Mo, W, Sn, but also Ti, V, Ni, Cr, or rare earth elements (REE) (Fig. 1). In contrast, the original metal content in the source rocks, i.e. the initial melt, ranges from ppb to ppm (Fig. 2). When comparing the two preceding figures, the metal enrichment spans about 4 to 5 orders of magnitude, increasing from the lithophile, siderophile to platinum group elements (PGE). Identifying the causes of metal enrichment is still a matter of debate underpinned by numerous models deriving from field observations, experimental studies or numerical simulations. None of which address the full complexity of the metal concentration process, either during the magmatic stage, nor during the late hydrothermal stage leading to ore deposits (Vigneresse, 2019).

An abundant literature, including research papers and textbooks, describes ore bodies of magmatic origin and their associated metal concentrations (e.g. Robb, 2004). Host intrusions are either granitic to dioritic in composition, as is the case for porphyry-type deposits (Sillitoe, 2010), ultramafic and alkaline (Barnes and Lightfoot, 2005; Maier and Groves, 2011), or even carbonatitic (Zaitsev and Bell, 1995; Mitchell, 2005). The body of literature also provides excellent detail with respect to the emplacement and evolution of the causative intrusive bodies, here simply called magma reservoirs (Edmonds and Woods, 2018), subsequent establishment of hydrothermal circulation systems leading to intense alteration patterns surrounding the causative intrusions, vein formation and the precipitation of metals. Models have been formulated for both barren and mineralized intrusions, and recently profoundly evolved from the so-called melting, assimilation, storage, homogenisation (MASH) model (Hildreth and Moorbath, 1998) in which the magma statically evolves by chemical differentiation (Štemprok, 1982; Breiter et al., 1999; Kemp et al.,

2007).Furthermore,mafic and ultramafic intrusions should involve a more complex scheme of chemical differentiation to explain how mineralizarions develop (Brassinnes et al., 2005). This paradigm of magma reservoir evolution recently shifted toward a far more dynamic system, with successive intrusions of different magma types, based on chemical grounds (Lee et al., 2014) and/or physicl and thermal considerations (Vigneresse, 2008; Annen, 2009). It constitutes the m-(M-SAE), acronym that includes a mantle participation and multiple intrusions from melting, segregation, ascent and emplacement. Magmas, with different composition, subsequently interact with the ambient stress pattern (Vigneresse, 2008). An additional fluid phase, immiscible with the silicate melt, should also be considered since it represents a supplementary possibility for the fate of into the magma reservoir.

The relation between igneous intrusions and metals generation as ore deposits has long been observed and described from the field as evidenced by an abundant literature. Large base metals concentrations in porphyry-type deposits along the Pacific coast of Chile and Peru provide evidence of their genetic relationships with granitic to dioritic intrusions. They have been described in great detail and exploited for hundreds of years. However, models of their genesis fail to fully explain how metals segregate and are enriched by several orders of magnitude. Often, metal concentration is attributed to late hydrothermal circulation (Sillitoe, 2010). At the same time, geophysical surveys have given further insights into the underlying intrusive and ore-forming processes. However, the two approaches differ profoundly in their methods and modes of interpretation and are rarely combined and integrated in academic studies.

The present paper reviews the types of modeling underlying the formation of magmatic ores in the context of porphyry systems. It is organized as follows: (i) first we provide a short introduction on the physico-chemical interactions between the major phases entering a magma reservoir. (ii) Then the various types of modeling (Tarantola, 2005) are examined (Fig. 3

First, we consider a direct problem, i.e. Lagrangian or Eulerian approaches, according to the adopted point of view on the parameters and measurables. Inverse problems are less developed in ore genesis, but are of common use for interpreting geophysical prospections on intrusions (Vigneresse, 1977; 1990). Finally, iterative processes, include non-linear differential system andor reaction diffusion equations (Fig. 3). (iii) A general model for ore generation is suggested, using both direct and inverse formulation., (iv) The discussion lists the inherent problems linked with modeling. It also examines the relationships between modeling and exploration.

2. Physico-chemical constraints

A model, to be valid, should represent both observations and/or experimental results.It should also possibly offering predictive solutions. Here the whole acting process of metal segregation, concentration and transportation before precipitation is simply called a system. . The controlling parameters of the system are inherent to the construction and evolution of a magma reservoir. For simplicity, only porphyry-type deposits are reviewed, and the immiscible phase, mostly aqueous, is called the magmatic volatile phase (MVP). Ore generation in a magmatic context follows the usual scheme of intrusions evolution, with a pronounced competition between melt and MVP. Consequently a similar modeling, with more or less chance, applies to barren or ore-related intrusions.

2.1. Phases in presence

A magma reservoir is built from successive intrusions of magma, the composition of which may vary according to the source, degree of melting and chemical differentiation (Vigneresse, 2008; Annen, 2009; Lee et al., 2014; Edmonds and Woods, 2018). Magmas result from successive inputs of mantle and/or crustal melts, i.e. with contrasting temperature

and composition, including fluids. The chemical evolution of the melt, strongly buffered in oxygen and sulphur, damps those inputs through hybridation (Castro et al., 1991). Although melting is continuous owing to temperature influence, melt segregation and ascent are discontinuous, due to the ambient stress pattern (Vigneresse, 1999, Rabinowicz and Vigneresse, 2004). When crystallizing, the magma reservoir registers such chemical variations, either by distinct mineral facies, the contacts between them, as well as their internal magmatic structures often displaying sharp contacts.

The magma reservoir presents three major physical phases. Those are the viscous melt from which crystals develop and form a solid phase or mush, and an immiscible MVP. Metals can also be considered as a supplementary phase, without distinguishing between metals for simplicity. They are initially within the melt, with the possibility to stay in it or to migrate toward the solid or volatile phases, according to partition rules.

Physical processes rule the bulk thermal evolution of the magma reservoir. They include heat diffusion, as well as viscous melt motion. The latter redistributes heat and metals that are still within it. Chemical partitioning of metals rules their transfer between the melt and either the MVP or crystals.

2.2. Interactions between phases

Interactions between the major phases should be examined separately whether they include metals or not. Melt motion has to face the mush (> 50 % crystals) that increases tortuosity (Boudreau, 1996). Tortuosity also affects the MVP motion, more mobile than the melt. Indeed, MVP first forms bubblesthat coalesce to form tubes that can slightly displace the loose solid framework of the mush (Huber et al., 2012). Nevertheless, feedback loops

between parameters (e.g. melt motion and mush development) characterize the rheology of cooling magma (Burg and Vigneresse, 2002).

2.3. Fate of the metals

Metals are initially in the melt as ionic components moving through diffusivity around 10^{-12} m^2/s (Zhang et al., 2010). They may integrate first forming crystals, according to a partition coefficient that takes into account their charge and ionic radius (Blundy and Wood, 2003). Once within the crystalline network, they still diffuse within the solid with diffusivity slower by about 6 orders of magnitude (10^{-18} m^2/s). Consequently, their diffusion length in crystals does not allow much travel (1 mm/My) within the life time of the magma reservoir. They can be considered as inert after integrating crystals. Metals may also stay within the viscous melt or integrate the MVP. The MVP composition (H_2O, CO_2, S, F and Cl) is essential to attract metals, owing to its difference in chemical potential with the melt. Metal enrichment in high temperature fluid and melt inclusions (Zajacz et al., 2008; Seo et al., 2009; Campos et al., 2009), in volcanic fumaroles (Zelenski and Bortnikova, 2005; Nadeau et al., 2013), or observed during experiments (Pokrovski et al., 2008; Lerchbaumer and Audétat, 2013), points to a magmatic origin for metals into the MVP. The MVP is also under supercritical regime, thus allowing infinite solubility for metals.

2.4. Metals deposition

With ongoing crystallization, mush develops that taps the MVP. When the MVP internal pressure overcomes the lithostatic pressure, the MVP is free to carry metals toward the surface, outside the magma reservoir. Metals precipitate, according to their solubility that drops when switching from lithostatic to hydrostatic and from supercritical to critical regime. Metals may combine with other elements to form oxides, S-compounds or halogen salts,

leading to complex molecules. The final formation of ore veins is enhanced by such late hydrothermal circulation.

Because metals enrichment from the melt toward the MVP,enriched MVP ascent and late brecciation are continuesly succesing in time, the tapping and brecciation of the overlying caprock repeats several times, leading to multiple deposition centers, as observed in the field. Join to this sudden liberation of the fluid phase, alteration aureoles develop, that represent a good tool for ore prospection. The important point here consists in the magmatic enrichment of the fluid phase in metals, with a cyclic nature of ore centers generation.

2.5. Implications

From this summary of ore formation, the whole system appears complex, with competing diffusion and advection. It requires examining a multi-phase material, continuously evolving with time in nature and abundance, thus hardly tractable through usual equations of mass and momentum conservation. In addition, the process is cyclic, with an unknown number of cycles, each varying in its components, physically and chemically. This means that feedback loops are numerous, with potentially unknown consequences.

The whole modeling should emphasize metals segregation and concentration from the melt toward the immiscible MVP. It should also consider melt and MVP motions. They constitute the physical aspect of the process. The chemical aspects consider metals partitioning between the phases.

3. Modeling

Modeling may involve either a qualitative or a quantitative approach. It usually starts from field observations and/or experimental measurements on the inferred parameters suspected to control all processes. Their determination is hampered by the conditions of observation, hence the initial inputs to modeling. Indeed, observables are a final snapshot of all undetermined processes that have previously generated the final aspect of a magma reservoir and ore deposit. They fall to determine all preceding transient situations. In addition, and that is not the least trivial character of the modeling, uncertain parameters, such as interactions between them and feedback loops, are unknown and/or not identifiable. Such a situation is common to all types of modeling, but often omitted by simplicity by modelers.

The modeling often consists in solving a system or a set of analytical equations, e.g. mass or momentum conservation. They may be linearized and/or solved using numerical methods of optimization. Such models usually provide numerical values on the amount of elements transfer.

Data processing and modeling commonly use top-down or bottom-up strategies. They are also known as direct and inverse problem (Fig. 3) solutions (Vigneresse, 1990; Tarantola, 2005). A third class of models approximates more complex systems, e.g. involving many non-linear interactions or feedback loops. It requires different approaches, often iterative, such as reaction-diffusion equations (Fig. 3).

3.1.Direct problem

In a direct problem approach, the measurements are used as such, and the modeling tries fitting to them by a judicious choice of the controlling parameters. There are no real mathematic criteria on the way the results should fit the measurements. In addition, two different approaches exist for examining the modeling (Fig. 4). The former involves an

Eulerian formulation, often through differential equations for mass and momentum conservation, or dynamic motion of the major parameters. Conversely, the second approach, or Lagrangian, considers the system of parameters from an external point of view. It is better designed for a qualitative analysis of the parameters influence. The two approaches differ when considering their derivatives. In the Eulerian system, $\partial/\partial t$ is the rate of change with time of the fluid property. It generally includes a term accounting for convection. Conversely, in the Lagrangian approach, D/Dt represents the acceleration of an individual element as it speeds up or slows down during its motion (Fig. 4).

3.1.1. The Eulerian approach

Analytical equations, or differential systems, describe the behavior of one particle (Fig. 4) using an external reference frame (Teschl, 2012). The system my decompose into more detailed sub-systems. Nevertheless, this decomposition may fail to identify the responsible mechanisms, since it is imposed as a prerequisite.

In the case of ore deposits, the Eulerian approach has been used a long time ago, mostly derived from hydrodynamic flows (Ague and Brimhall, 1989; Garven, 1995; Cathles and Adams, 2005). Models have first been developed in 1D for simplicity, before increasing computing power led to 2D and 3D simulations. They take the form of particle or fluid motion according to hydrodynamic concepts (Chi and Xue, 2011), e.g. through an inspection of the driving forces, fluid pressure regimes, fluid flow rate and directions to localize metals concentration. The inputs may also involve the larger scale tectonic environment, topographic variations due to erosion, or tectonic deformation. Such factors have influence in changing the local stress pattern thus modifying the fluid pressure and the veins pattern. introducing the equations of heat transport, mass and momentum conservation (Ju and Yang, 2011), examines a more complex situation. In the former case, the model allows investigating the role of

external factors such as the effect created by an unconformity surface, with meteoritic water infiltration through dipping faults, on the thermal inputs during ore genesis. Introducing the analysis of the fluid pressure regime and the flow rate provides insights on the driving forces that control cooling and salt content in mineralizing fluids (Chi and Xue, 2011). The equations of mass and momentum transport, coupled with the heat equation examine the effects of replenishment by the successive injections of new magma (Schöpa and Annen, 2013). The time delays between intrusions are essential to insure the fate of the intrusion. Hence too large volumes of intrusions or too short delays between them fail to produce large reservoirs of mobile magma because a large quantity of mush has no time to develop. A model, specifically dedicated to the Yerington Batholith, Nevada, has been constructed (Schöpa et al., 2017) for modeling its three successive magma pulses. It results that magma should be emplaced at a high rate (> 4 cm/yr), uncommon in plutons, but with periods of quiescence between them exceeding 100 kyr. Coupled interactions between magma intrusion and cooling modify the local regime of deformation, rearranging the brittle-ductile transition, with implication on the development of fractures (Guillou-Frottier and Burov, 2003; Zhang et al., 2011

In such models of porphyry-type deposits, the zone under study is first discretized spatially through a triangular or rectangular grid, the spacing of each node being of the order of 50 m. A supplementary discretization in time allows to reproduce the incremental emplacement of successive magma inputs (Schöpa et al., 2017). The discrete volumes of magma have their own composition, i.e. temperature and fluid content. It simulates the incremental growth of a granitoïd intrusion. Discretization also allows computing the required derivatives, in space and time that rule the system of equations for magma flow, fluid motion and heat losses. Successive models using different time interval for the new magma inputs investigate the role of magma residence time. They provide constraints on the thermal

evolution of both the magma reservoir and the mineralized fluid release (Chelle-Michou et al., 2017; Schöpa et al., 2017). Nevertheless, several successive direct models are required, examining the controlling parameters (delay between intrusions) to conclude for an acceptable model. The overall impression is that a long error and trial process should first identify which parameter better control the system. This suppose that they are all identified, excluding possible feedback loops. A similar approach, using temporal evolution is also matter of modeling, using U–Th–Pb–He time–temperature data (Fu et al., 2010). The model identifies a first phase of cooling while the surrounding rocks are heated. A following stage assumes cooling of the whole system and corresponds to exhumation of the intrusive. The same approach, focusing on the nature and intensity of the stress pattern, determines fractures evolution around an intrusion, examining the position of the brittle/ductile transition (Weis et al., 2012). The released fluid, enriched in metals, may serve as an estimate to the quantity of specific metal, e.g. copper, that can be extracted from the intrusion. Enrichment by a factor of 1000 is something obtainable in a 2D simulation, using a 10 by 3 km magma reservoir of elliptical shape with a cupola in the roof at 5 km depth (Weis et al., 2012).

Chemical exchanges have been examined on chemical bases through simple chemical reactions and evolution, using trace elements for instance (Wright et al., 1983). Further developments apply to specific minerals, e.g. REE fractionation in apatites (Krneta et al., 2018), trace element zoning in accessory minerals (Melnik and Bindeman, 2018) or more simply to trace elements fractionation (Tauson et al., 2018). Similarly, fluid-rocks interactions studies started from mineralized fluid flow in porous or fractured medium (Steefel and Lichtner, 1994; O'Brien et al., 2003) and leaching metals from the country rocks (Mouhers, 2015; Myagkiy et al., 2017). Such studies apply to porphyry type deposits (Weis et al., 2012) in relation with geodynamics (Liu et al., 2008) or environmental problems (Zhao et al., 2014). They show that ore develops as a consequence of dynamic variations in rock permeability,

mostly driven through the injection of fluids released by adjacent magmatism. Hence, a static permeability cannot reproduce the observed alterations, whereas a dynamically driven permeability in response to magmatic fluids creates a metal-precipitation front leading to potential metal enrichment, such as Cu, up to a factor of 2000 (Weis et al., 2012). Nevertheless, the authors recognize that the mechanism of fluid extraction from the magma remains a major unknown in the model.

The solution of the system of equations may be avoided, using non-dimensional numbers that characterize the structures or patterns of the solutions. This is done through non-dimensional ratios of the acting parameters. Associated to them, a wavelength determines the geometric parameters, providing a geometric constraint on the metric associated with the solutions. They determine the type and shape of instabilities (see review in Vigneresse, 2015). Among them, the Reynolds number (Re) ratio of inertial forces to viscous forces, the Stefan (St) ratio of the sensible heat to the latent heat, and the Péclet number (Pe) ratio of advection to diffusion. At last, the compaction length (λ) determines the average spacing of melt veins during segregation (Rabinowicz and Vigneresse, 2004). Such numbers are essentially qualitative for determining the instability pattern resulting from the competition of two essential parameters.

3.1.2. The Lagrangian approach

The Lagrangian approach (Fig. 4) involves indirect methods, such as cellular automata (CA), lattice gas automata (LGA) or lattice Boltzmann modeling (LBM). They are mathematical abstraction of a physical system (Chopard and Droz, 1998) after its discretization in space and time. The space is divided in small finite cells, whereas the time evolution is represented by the successive states of each cell. Such methods (CA, LGA or LBM) are used to represent complex physical situations, in which a direct Eulerian solution is

hardly tractable, when the geometry or amount of each phase vary continuouslySuch examples of CA include partial melting in migmatites (Vigneresse and Burg, 2000; 2006) whereas LGA are widely in use for reactive fluid (Kang et al., 2006; Pazdiniakou et al., 2018) or fracture propagation (Marconi and Chopard, 2003). More complex interactions have recently been addressed to simulate metals segregation within a mush, with a viscous melt and a loose rigid framework (Huber et al., 2008; Parmigiani et al., 2014).

CA have first been proposed by von Neumann (Burks, 1970) and the model has been popularized with the advent of computers (Wolfram, 1983; Toffoli and Margolus, 1987). The space and time discretization inherent to CA totally differs from the discretization of the partial differential equations representing the physical process. Hence CA mimics the physical interactions between adjacent cells and the time evolution of the system is given by the successive states they adopt. Each cell presents a finite number of states, indicating its major physical state, for instance the finite percentage of melt in case of a rock under melting (Vigneresse and Burg, 2000). CA is by essence deterministic. Models only require integer values, making their numerical implementation exact (Chopard and Droz, 1998). A rule, representing the interactions between cells mimics the imposed geometric conditions of motion (e.g. under strain). Since the discretized space is finite, its boundaries are commonly periodic to avoid jamming, assuming mass conservation within the system.

The use of CA in solving complex problems has a two-fold expression. First, the model can predict the physical properties of the considered system. However, the quantification of the system is hampered by the scaling, and can predict only relative values, according to the imposed rule. For instance, in migmatites an imposed shear strain is more effective in displacing the mobile melt than vertical compaction or pure shear (Vigneresse and Burg, 2006). Second, the CA method informs on the consequence of an imposed rule. For instance, during melt extraction in partially molten rocks (Vigneresse and Burg, 2000), the

mobile melt within a solid matrix moves under simple or pure shear. Indeed, strain preferentially partitions into the mobile melt. Two threshold values are fixed, the first for melt motion, and the second ruling the possibility for the melt to escape the system. They are fixed according to field observations (Vigneresse et al., 1996). Nevertheless, the CA model allows bracketing such thresholds below which the melt motion cannot connect cells, or above which a too loose framework results in a rapid melt escape and drying of the molten rocks. Thus, the modelling serves as a qualitative determination of the parameters and examines their consequences on the physical or chemical evolution with time. It clearly demonstrates in case of rocks melting, that melt extraction proceeds due to the ambient stress pattern. Simple shear moves the melt whether pure shear concentrates it. An important point is also the discontinuous character of melt extraction, observed in both Lagrangian and Eulerian formulations (Vigneresse and Burg, 2006; Rabinowicz and Vigneresse, 2004).

In a cellular automaton simulating metal enrichment in a mushy magma reservoir, time and space are discretized through finite particles. Space is represented by a finite number of cells on a 2D or 3D periodic lattice. Each particle is assigned to a physical phase component, e.g. melt, fluid or solid. Each cell has a fixed number of possible eigenvalues ranging from 0 to 100, which mimic its metal content. Initially the metal is entirely randomly distributed in the melt. Rules control the distribution and motion of the cell content with time. Metals may enter the solid phase in a restricted percentage, whereas it is enhanced to enter the volatile phase, thus mimicking the partitioning. The cells representing the melt and the MVP are free to move, according to their ability to flow, fluid being more mobile than the melt, though a crystal mush slows down both motions. Bubbles accumulation has potential importance in determining the eruptability of magmas (Parmigiani et al., 2016).

Lattice gas automata (LGA) or Lattice Boltzmann modeling (LBM) represent a subset of CA, more designed to describe hydrodynamic processes as discretized kinetic models

(Chopard and Droz, 1998). The system is also discretized in 2D or 3D space (Fig. 5) and internal rules mimic the discrete motion of the particles. In particular, it quantifies the interactions between cells, using an intrinsic value attached to each cell. This profoundly differs from CA methods. It has importance in determining the state of the cell after collision, whereas a simple propagation does not provide any information from outside the domain. The same way as in CA, the boundaries incorporate either periodic or kinetic (Animali and Karlin, 2002) conditions. In general, LBM also allows more flexibility than CA on complex boundary problems.

For hydrodynamic problems, LBM represents a more efficient method than the usual Eulerian approach though Navier-Stokes partial differential equations (Suga, 2006; Shan et al., 2006; Pazdiniakou et al., 2018). It has also advantage on the Eulerian formulations in complex convective problems, since it may incorporate phase changes (Huber et al., 2008; 2012). The ability of each cell to have its own predetermined state also represents a valuable advantage when dealing with complex interactions between cells of contrasted properties (e.g. between fluid and solids, or solids and gas) in a porous media (Pazdiniakou et al., 2018).

Commonly, the Lagrangian approach provides better information in complex systems compared to an Eulerian formulation. However, the quantification of such results remains difficult to calibrate. At least, the direct problem formulation is deterministic, providing a solution that strongly depends on the initial imposed conditions. Successive models, with one parameter changed at each time, allow identifying which effect results from the changes. It does not allow identification of any unsuspected cause or feedback loops.

3.2 Inverse problem

During inverse problems, the measurements are used to deduce the controlling factors ruling the system (Tarantola, 2005) (Fig. 3). This supposes that qualitative and quantitative

relationships exist that connect the parameters to the results, even when such equations are approximate. Equations may be linear, leading to a system of equations easily solvable by matrix inversion, or non-linear. In such a case, appropriate methods, often iterative such as the steepest gradient (Arfken, 1985), should converge toward a solution. Basically, it is equivalent to linearizing the system by successive approximations. The following review mostly focuses on linear systems.

3.2.1. Linear systems of equations

A system of equations would it be linear or not relates the number of pertinent equations (m) in the vector **m** to the vector **x** with (n), the number of unknowns (n), through a matrix **A** (Fig. 6)

$$\mathbf{m} = \mathbf{A}\,\mathbf{x} \qquad (1)$$

The system is considered as underdetermined when there is less equations than unknowns ($m < n$). Conversely, it is overdetermined when there are more equations than unknowns ($m > n$). Hence, each unknown can be viewed as a constraint, restricting the degree of freedom of the system (e.g. Trefethen and Bau, 1997). But the above definition suffers many exceptions, linked with the rank of the matrix, rk(**A**), that identifies the number of linearly independent columns or rows of the matrix. Suppose a huge set of equations measuring the temperature, chemical composition and amount of a given metal (e.g. copper) in a single ore deposit. Such measurements have been realized on a grid with 1m spacing, over a zone 10 by 10 km wide. The number of equations (measurements) is thus largely greater than the number of variables (e.g. 3). The system should be overdetermined, according to the above definition. But most equations do not provide enough information on the global evolution of the ore deposit. Certainly, some obvious parameters (fluid conditions, time, etc) are lacking from the three imposed variables. The information carried by the set of equations

is thus redundant, and non-informative. The system is underdetermined. This is actually the case when all variables have not yet been identified, or when the number of observations (the number of equations) does not reflect the action of all varying parameters, as it is the case for feedback loops. Such a situation has been pointed out (Atlan, 2011) and frequently occurs in biology, where emergence and auto-organization come out from complex situations. The situation manifests by the possibility of several models, with different parameters, to adequately fit the measurements.

The simplest problem occurs with a square matrix **A** (m = n). Specific numbers quantify the matrix **A** (e.g. Howard, 1984). First, the rank of a matrix rk(**A**) corresponds to the maximal number of linearly independent columns, indicating redundant information (Fig. 6). Then, its eigenvalues (λ_i) satisfy the eigen-equation $\mathbf{A} - \lambda \mathbf{I} = 0$, in which **I** is the identity matrix (all terms null, except those of the diagonal fixed at 1). Their full set of eigenvalues forms the spectrum of the matrix, Sp(**A**) (Fig. 6). The trace Tr(**A**) is the sum of all eigenvalues, whereas the determinant det(**A**) is their product. At last, the condition number of the matrix κ(**A**) is the ratio of the maximum to the minimum eigenvalue (Fig. 6). In case of a system of equations, the Jacobian matrix (**J**) designs the matrix of the partial derivatives of the system. It determines the stability of the system. Numerically, the solution of a square system (m = n) should be unique, provided the rank of the matrix is also equal to n, i.e. there is no redundant measurement. This ideal case manifests by n eigenvalues distributed along a spectrum, or not invertible scalars. The case of underdetermined system manifests by a region in which solutions best represent the measurements. It signifies that there is more than one solution. A minimal length solution determines a specific solution that has a minimum squared norm. In this case, the spectrum of the matrix has all finite values (Trefethen and Bau, 1997). (Fig. 6) When the matrix is rank deficient, a pseudo-inverse can be computed using a

decomposition in singular values (see below), involving a damped least-squares process (Vigneresse, 1978).

The most common case is overdetermined. A solution exists relying on the norm chosen to minimize the errors on the solution. In a one-dimensional case, the so-called L_1 norm corresponds to the median, or least absolute value of the error bar. Conversely the L_∞, or Chebyshev norm, considers the maximum error. Commonly the least squares approximation, or L_2 norm considers the squared errors, equivalent to the usual mean square error. The most common method for solving any system in a least squares sense is by converting the rectangular **A** matrix into an invertible square matrix, just by multiplying both sides of Eq. 1 by the transposed $\mathbf{A}^T$ matrix.

$$\mathbf{A}^T \mathbf{m} = \mathbf{A}^T \mathbf{A}\, \mathbf{x} \qquad (2)$$

Although the method seems simple and easy to implement, it rapidly reveals complex when using numerical values. Indeed, the numerical values of the $\mathbf{A}^T \mathbf{A}$ matrix present extremely dispersed values, making the matrix ill conditioned (Lawson and Hanson, 1987). In terms of solution numeracy, the norm L_2 offers only one solution whereas L_1 offers many. Conversely the computational difficulty increases with L_2.

3.2.2. Singular value decomposition

Inverting the system in the sense of the least squares norm requires examining a singular value decomposition (Golub and Reinsch, 1970; Lawson and Hanson, 1987). Because the $\mathbf{A}^T \mathbf{A}$ matrix is by construction ill-conditioned, i.e. with eigenvalues displaying contrasted amplitudes, it is necessary to examine the spectrum of the matrix (Sp(A) or diagram of the eigenvalues) (Fig. 6). In particular, redundant equations bearing no additional information on the relationships between variables and measurements, mark by small to very small eigenvalues (Fig. 6). They should be removed from the final solution. But this implies

to compute eigenvalues and eigenvectors by some process of ranking. A first formulation uses a singular value decomposition. It directly starts from the **A** matrix, and by successive rotations, determines a diagonal matrix (**S**), with the required eigenvalues (Fig. 7).

$$\mathbf{A} = \mathbf{U}\,\mathbf{S}\,\mathbf{V}^{\mathbf{T}} \qquad (3)$$

The rotation matrices, **U** and **V**, are such that they do not modify the bulk dimensions of the system since their products by their transposed ($\mathbf{U}\,\mathbf{U}^{\mathbf{T}}$ or $\mathbf{V}\,\mathbf{V}^{\mathbf{T}}$) are unit matrices. The successive products are geometrically equivalent to a rotation and scaling along the eigenvectors (Fig. 8). The process is repeated for all eigenvalues. The columns of U and V form an orthonormal new basis for the system. The rank of the matrix equals the number of non-zero singular values which is the same as the number of non-zero diagonal elements in **S**. The eigenvalues of **S** are the squares of the eigenvalues of **A**. In that sense, they relate to the energy contained into the matrix. The singular value decomposition provides the pseudoinverse of a matrix, whatever its dimension (Vigneresse, 1977). A second step exists to take into account the low eigenvalues that contain few information. The Levenberg-Marquardt scheme replaces the inverse of the eigenvalues by a function with a damping parameter (Lawson and Hanson, 1987) that stabilizes the results (Vigneresse. 1978).

The singular value decomposition and pseudoinverse have been successfully applied to signal processing (Sahidullah and Kinnunen, 2010) and image processing (Sadek, 2012), In particular they are widely used for image compression (Andrews and Patterson, 1976). Other applications focus on large data sets, such as genomic signal processing (Alter and Golub, 2004). It should be noted that common spreadsheets providing least squares approximations do not take into account singular value decomposition and often lead to unconsistant results when used without discernement.

Inverse problems are not often used to understand the generation of ore deposits. It reflects the underlying complexity of the process, owing to the unhierarchised parameters that enter ore genesis (e.g; metal abundance, temperature, pressure, chemistry…). It does not allow a simple formulation from the observed manifestations (veins, brecciation), and can hardly cope with multiple centers of ore generation and the many metals involved (Landtwing et al., 2002; 2010).

Nevertheless, least-squares approximations are in common use for fluid inclusions characterization (Wilkinson, 2001) or geochemical trends appreciation. More commonly, extraction of anomalous mineral composition, especially trace or rare minerals are statistically examined in order to detect anomalous concentrations. Thus, analysis and discrimination between trace elements (Herrmann and Berry, 2002), or specific minerals, (e.g. magnetite) composition (Ghasemzadeh-Barvarz et al., 2016) are often inspected using least-squares investigations. Large geochemical data sets are also submitted to statistical trends for extracting the most probable places or regions of any geochemical concentration (Kun et al., 1987). Such simple applications are rather statistical than conceptual, in that sense that they provide evolution trends rather than identification of the genesis conditions.

Because the relations between measurements and parameters are more appreciated and quantified, geophysical methods commonly use least-squares based inversion methods to determine the shape, volume or extension of ore bodies from gravity data (Vigneresse, 1977; 1990; Dolgal et al., 2016). More generally, potential field methods offer also such possibilities of inversion (Malehmir and Bellefleur, 2009; Eppelbaum, 2014).

3.3. Iterative methods

In case of non-linear systems of equations, two general methods of solving use an iterative solution. From an initial approximation of the model, successive iterations tend to reproduce the measurements (Fig. 1). Non-linear algebraic equations can easily be reduced to a system of polynomial equations and solved through specific algorithms such as the Newton's, or Newton-Raphson's method or the steepest descent method (Arfken, 1985; Süli and Mayers, 2003). Iterative by construction, the solution generally converges toward a solution, giving place to a generalized inversion (Ben-Israel and Greville, 1974).

3.3.1. Non-linear systems

When the system is highly nonlinear, the approximation through pseudo-linearization often fails to correctly represent the underlying physics. Inverting a large sparse matrix or a non-linear system is equivalent to solve the intersection of a conic curve and a plane. The solution is generally non-unique, at least in two dimensions i.e. with only two variables. Still in two dimensions, it depends if the curve intersects, is tangent or does not cross the curve. When the dimension is higher, a system of non-linear equations describes the process. The variables, or unknown functions in case of partial derivatives, are represented by polynomial of degree commonly higher than one. When several variables simultaneously occur in such equations (e.g. x and x^2 or x^3) those can enter the systems as a new set of variables. The same is valid for simple derivative functions when their analytical expression is known.

The Newton's method is used if the number of equations is equal to the number of variables, rarely the case in fact. However, it does not provide all the solutions nor prove that there is no solution. A starting point constitutes the initial condition. The method has a better and faster solution when the initial starting point is close to a solution. The steepest descent is a gradient method for finding the minimum of a function through an iterative optimization algorithm. It has basis on Marquardt's method of minimization (Marquardt, 1963)

interpolating between a common Gauss algorithm and gradient descent to locate the minimum value of a surface, viewed as a potential low..

Those methods minimize the sum of the squares of the equations, thus pertaining to a least-squares approximation. Nevertheless, in case of several local minimum solutions, they may be estimated as global solution, avoiding the real global minimum. The methods work for overdetermined systems, but outputs an empty information if all local found minima are positive.

3.3.2. Other iterative solutions

Some non-linear equations provide a reasonable description of a physical process. Hence, the geophysical effects generated by a 2D or 3D body are easily modeled by direct methods. Such equations can be inverted, from an initial starting model, with arbitrary parameters, and then, iterative modifications provide effects that are compared to the measured effects (Vigneresse, 1990). The algorithm is quite simple, but some cautions should be provided on the convergence of the solution. Convergence is actually always realized, but it may lead to spurious effects. Such effects manifest by a convergence of the solution, i.e. a minimization of the errors between observations and computation, but also by a divergence due to improper input parameters. They consist in numerical instabilities that may serve to bracket the initial parameters into a range leading to convergence.

Such effects have been put in evidence during gravity data inversion to get the 3D shape at depth of granitic intrusions (Vigneresse, 1990). Hence, depending on the adopted values for densities distribution, two divergent types of solution (in the geological senses) are observed whereas the results numerically converge. When the input densities are too large, the computer deals with an excess of mass that does not fit the underlying real distribution of mass. The successive iterations compensate such excess by adding unobserved mass deficit

outside the physical limits of the intrusion. Conversely, when the densities distribution cannot yield the total mass, then the intrusion dramatically increases in depth, but compensates the mass deficiency by adding spurious reliefs aside. In both cases, the divergence of the results with observations helps in bracketing the values of expected solution (Améglio et al., 1997).

These divergences also occur during other iterative processes, attesting a mismatch in the input parameters with the real values. However, such numerical divergence is easily discernable and can be used to infer a better choice of the input parameters.

3.3.3. Reaction-diffusion systems

A simple chemical reaction transforming one atom of metal (e.g. Cu) into a salt fails to explain enrichment even through reactants. In usual chemical reactions, one atom of Cu is transferred from the melt toward the MVP, and there is no enrichment. To achieve chemical enrichment, the process requires that the reaction increases the amount of metal by a factor n, here about 3-4 orders of magnitude. Such enrichment in one variable is observed in systems of reaction-diffusion, as for instance, during the separation of pigments forming zebra stripes either in animal patterns or in zebra rocks (Murray, 1993; Kelka et al., 2017). It points to chemical amplifiers, or reactions involving several steps with successive enrichment in one element. Such reactions present non-linear positive or negative feedback loops, all describing oscillating enrichment, up to chaotic behavior, e.g. the Belousov-Zabotinski reactor (Gray and Scott, 1990; Benini et al., 1996) or the Brusselator (Nicolis and Prigogine, 1977). The latter is typical of autocatalytic reactions, increasing the concentrations in one element, with cyclic oscillations around a fixed point. The only possibility for such feedback loops to develop is through unstable reactions in contrast with steady state reactions as involved during fractional crystallization.

The starting equation is a simple 1D diffusion determining the evolution with time, using $\partial_t u = du/dt$, or a gradient of concentration $\nabla^2 u$ with diffusivity D_u while it is submitted to a local reaction R(u).

$$\partial_t u = D_u \nabla^2 u + R(u) \quad (4)$$

Depending on the local reaction non-vanishing with time, the equation may lead to the Kolmogorov time process (Kolgomorov, 1931) presenting an oscillatory state. The generalization to higher dimension gives place to systems of reaction diffusion in which an inhibitor (u) and an activator (v) compete, yielding the so-called Turing machine (Turing, 1937), an algorithm able to process first-order logic sequences within an unrestricted grammar. The system writes :

$$\partial_t u = D_u \nabla^2 u + R(u) \quad (5)$$

$$\partial_t v = D_v \nabla^2 v + S(u) \quad (6)$$

Pertaining to the same process, the Lotka-Volterra equations describe the interactions between a population of preys and predators (Lotka, 1910; Volterra, 1926; Arditi and Ginzburg, 2012). A couple of simple equations describes the growth and death of a prey population (u), whereas predators (v) grow and interact with the preys.

$$du(t)/dt = \alpha\, u(t) - \beta\, u(t)\, v(t) \quad (7)$$

$$dv(t)/dt = -\gamma\, v(t) + \delta\, u(t)\, v(t) \quad (8)$$

The rates of change in the populations with time are the derivatives du/dt and dv/dt. The coefficients of the differential system are the controlling parameters. In such equations, α is the growth factor of the prey population, equivalent to the gradient of concentration, and β the rate for a prey to meet a predator, γ represents the loss rate of the predators, or concentration

gradient, and δ represents the growth of the predator population. A good application works for rabbits and foxes (Arditi and Ginzburg, 2012). Thus, depending on the evolution rates of each population, catches and deaths, one population may take over the other (Holling, 1973). The interest of the system of equations is the possibility for one population to grow over its initial value, i.e. to show enrichment.

Interestingly, the stability of such differential systems is similar to the stability mapping, and analogue to a Poincaré map, of viscous flows during deformation (Manneville, 1991; Iacopini et al., 2010; Xypolias, 2010) that have recently been reviewed (Vigneresse, 2015). The mapping uses the determinant (det (**A**)) and trace (Tr(**A**) of the matrix describing the system. The value of the determinant separates both hyperbolic flows (det(**A**) < 0) from non-dilatant flows (det(**A**) > 0), and source (Tr (**A**) >0) from sinks (Tr(**A**) <0). In between, when 4 * det(**A**) - Tr(**A**)^2 = 0, the flow is parabolic. Another parameter, the spectrum of the matrix (Sp(**A**) determines the flow stability, provided Sp(**A**) < 0 (Fig 10). The Poincaré mapping commonly plot the successive solutions within appropriate coordinates, thus illustrating the cyclic nature of solution and its eventual attractors (Iacopini et al., 2010; Xypolias, 2010).

The so-called Gray-Scott scheme generalizes such iterative models. It describes a chemical conservative equation under which the source (U) and drain (V) result in a product (P) under the chemical equations U + 2V → 3V and V → P (Gray and Scott, 1990). Under such conditions, the two reactions R(u) and S(u) in Eqs 7 and 8, simplify into

$$\partial_t u = D_u \nabla^2 u - u\, v^2 + F(1-u) \qquad (9)$$

$$\partial_t v = D_v \nabla^2 v + u\, v^2 - (F+k)\, v \qquad (10)$$

When considering only the first right hand term of Eq. 9, it is equivalent to the heat equation. The term in ($u\ v^2$) is the reaction rate, whereas the term in F(1-u) represents the replenishment and v is the diminishment term. The two constant values F and k represent the feeding rate and the kill rate respectively. The results strongly depend on the two constants F and k, showing no reaction at all when F is either null or too high. In between oscillations occur, that may yield to chaos. Such changes in the resulting patterns have been considered as bifurcations in the number of solutions which can be analyzed through the Jacobian of the system (Eqs. 9, 10) (Hale et al., 1999). Indeed, it presents two eigenvalues, namely -F and -(F+k), that determine a trivial critical point (Delgado et al., 2017). A mapping of the types of solutions is constructed (Fig. 10). It uses the trace and determinant of the Jacobian, matrix of the first derivatives of the system. The diagram separates the points of bifurcation from the stable solutions of the system.

When such models were issued, they gave place to an abundant literature, mainly focusing on bifurcations of solutions, leading to chaos (e.g. Glendinning, 1995), but also to self-organization (Ortoleva, 1994). They found rapid applications in chemical systems presenting oscillations with time. Other applications include pattern formation due to two competing diffusion processes, such as stripes (Murray, 1993), or pigmentation patterns on mollusks shell (Meinhardt, 2009; Kelka et al., 2017), and more often in rhythmic ore alternance (Shahabpour, 2005).

Liesegang bands and oscillatory zoning have also been interpreted with such competing diffusive process (L'Heureux, 2013). Layered intrusions and orbicular rocks, as well as oscillatory zoning in plagioclase could be manifestations of such a double diffusion process. A former model of ore generation had been constructed using the Gray-Scott model (Yu, 1988). The model starts indicating that ore-forming pertains to dissipative structures as earlier formulated (Prigogine, 1978), i.e. pointing to an open system, probably far from

thermodynamic equilibrium, with continuous exchange of matter and energy. It rules out most direct Eulerian models, in which stationarity is implied. But the paper (Yu, 1988) becomes unclear on the time scale of the so-called dissipative structures, examining periods of formation starting in the Cambrian up to Cretaceous. Identically, it is not clear on whether the metals are coming from, intrusion or sediments.

The concepts of reaction-diffusion have been recently applied to ore generation, aiming to show a cyclic behavior in metal enrichment (Oberst et al., 2018). The starting point is the initial distribution of mineralized veins in drill cores. A differential system is built that mimics the reaction-diffusion process, using different diffusivity values for the inhibitor and the activator, the latter being about the double of the former, as commonly implemented in a Gray-Scott model. The results show a discontinuous, but cyclic and non-periodic distribution of the veins. Such approaches exhibit many features of nonlinear dynamical systems, especially when the system is brought far from its natural equilibrium. Then feedback relationships between thermo-chemical and deformation processes produce recurrent fluid temperatures and pressures fluctuations leading to the deposition of mineral veins. It roughly corresponds to the distribution of minerals, such as carbonate amphibole and sericite with a spatial occurrence increasing in this order (Oberst et al, 2018). Nevertheless, the study was aimed to show the applicability of such reactions to simulate the distribution of ore, but not aimed toward the mode of concentration of associated metals. Such models should be used in case of rhythmic layering, e.g. chromite layers from the Bushveld (Cousins, 1959; Kinnaird et al., 2002) or any banded iron formation (Klein, 2005).

4. Provisional conclusions on modeling

The preceding review rapidly described the three types of modeling, identifying direct, inverse and iterative problems (Fig. 3). Each of them results in solutions that should be compared in terms of pertinence and representativity, which is often omitted.

4.1.Pertinency and accuracy of models

Difficulties during modeling consist in estimating the accuracy and, above all, the pertinency of the constructed model. Accuracy mostly relies on the quality of observations, depending on their spatial distribution and on their temporal evolution, when available. The latter is often unknown since measurements mostly consist in late snapshots of the process, when they are not obliterated by tectonics or alteration. Consequently, a direct approach can hardly represent the temporal evolution of ore generation. In particular, it cannot integrate the cyclic nature of ore genesis, excepted by determining successive quasi-stationary models with time (Weis et al., 2012). Historically, the direct 2D formulation has been the first approach in geophysics with the decomposition of the source bodies in polygonal bodies (Talwani et al., 1959), rapidly followed by 3D modeling in gravity and magnetism. The offered solutions were directly compared to field observations. Varying the leading parameters brackets the output values, i.e. identifying a possible hierarchy between the inputs. This is a first step in the understanding of the underlying processes. However, the unique solution provided by the overdetermined system remains strongly function of the input parameters. When one of those is omitted or underestimated, or when feedback loops develop, the given solution fits the input, but hardly the reality of the processes.

In order to avoid more uncertainties, inverse modeling has been introduced in the early 70s. It has been imposed by the huge amount of new data released from geophysical surveys and the introduction of large computing facilities. Models first concerned global structures, such as the internal structure of the Earth, as deduced from its free oscillations or bodies

surveyed for their electric, gravity or magnetic disturbance (Backus and Gilbert, 1970; Parker, 1970; Wiggins, 1972). It gave place to a general inverse formalism, factoring the system through its eigenvalues and eigenvectors (Franklin, 1970; Gilbert, 1971; Jackson, 1972). The formalism came out from the common observation that an ill-posed matrix of the equations should provide spurious inverse matrix (Eq. 2). Optimization between the resolution of the data, the expected errors in the solution and the fit of the data had to be taken into account. It led to tests conducted using different norms such as the sum of the absolute errors or the sum of the squared errors, thus mimicking the L_1 and L_2 norms, with the advantage of the latter that needs less delicate computation (Vigneresse, 1977). In fact, this problem goes back to the 17th century with the dispute about the shape and size of the Earth between Boscovich and Laplace in one hand against Legendre and Gauss in the other one (Tarantola, 2006). Nevertheless, such formulations commonly provide solutions, often a set of them, from which statistical tests should identify the best fits.

The dichotomy between over- and under-determined systems is often ignored during modeling. In the direct, or forward problem, one solution only exists, due to the causal principles. But this solution strongly depends on the input parameters that are not necessarily adequate or exact. In contrast, the inverse problem may present several solutions, resulting from similar observations or measurements. It may also present no solution at all in case of inconsistent data. In case of many solutions, f.i. in case of very underdetermined system due to the high number of parameters, the many solutions can be compared with prior information, resulting in equivalents error bounds when fitting to the observations. Such solutions are called equivalent. The key to solve such ill-posed problem consists in analyzing the eigenvalues of the system (Wiggins, 1972), i.e. decomposing the matrix of the system into its singular values (Lawson and Hanson, 1987). At least, it reinforces the strong formalism that underlies the inverse problem (Backus and Gilbert, 1970). Nevertheless, it does not solve

the non-unicity of the solutions.

4.2. Heading toward a direct, inverse or iterative problem

It remains to select between a direct and an inverse formulation, i.e. between a unique solution but dependent of many a priori arguments, and many solutions compatible with the observations. Uncertainty exists due to a poor calibration of the initial data and noise during measurements and discrete sampling. This relates to the data themselves. Approximate conceptualization of the underlying physics, model physical assumptions (e.g. homogeneity, isotropy), linearization and numerical approximations restrict the validity of the model. The equivalent models fitting the observations within the same error bounds, and resulting from both successive direct computations and inverse modeling, are located within curvilinear valleys called the cost-function topography (Fernández-Martínez, 2015). The choice between such equivalent solutions is totally arbitrary, and there is no statistical way to identify one of them that would correctly explain the observations.

The use of an iterative solution is hampered by the choice of the initial parameters. In particular, the rates of growth or of decay are totally out of constraints. For ore deposits, a few constraint exists on the MVP exsolution (Edmonds and Woods, 2018), that can be checked through bubbles nucleation and growth. But it does not inform on the rate of metal incorporation into the bubbles.

In practice, modeling ore deposits commonly uses the direct formulation, whereas geophysical surveys prefer using an inverse problem. Certainly, this relies on a stronger physical formalism underlying geophysical methods. Since the parameters in cause for metal segregation are physical and chemical, thus internal to the way under which the magma reservoirs evolve, it has been tempting to determine how such tuning develops, on a broad

scale, leading to so-called “magmatic provinces” (Petrascheck, 1965; Sillitoe, 2010) and on local scale, yielding barren and/or mineralized intrusion.

5. Toward a general model

Basically, the generation of ore deposits is a competition between gradients (e.g. section 2). Those are the gradient of concentration, the gradient of velocity between a flowing melt, a moving fluid and a quasi-rigid crystal framework, and the gradient of metal partitioning between the melt and the MVP. They all result in metals enrichment by a factor 10^3 to 10^4, which is huge.

5.1. Addressing the right questions and providing the right answers

The major parameters leading to ore generation within intrusions have been identified (see section 2). Therefore, any modeling that would examine the variations of these parameters would be some modification of a direct problem (section 3.1), i.e. involving an overdetermined system, with inherent multiple acceptable solutions (Atlan, 2011). A full analytical inverse formulation is presently ruled out because of inherent feedback loops between advection and diffusion. The problem of ore generation must be reformulated to address the right questions on the manner and quantity metals are enriched (Vigneresse, 2019). But the answer to such questioning is certainly not simple. An inverse formulation based on the input parameters such as ore grade, temperature, melt and fluid composition requires too many poorly constrained values. The changes in the physico-chemical properties of the melt-crystal-fluid system is also hampered by their continuous evolution in both space and time. At last, metal chemistry offers so many complex associations with ligands, even simple (S, halogens) that it is hardly tractable.

5.2. Background of the model

The suggested model is a mix between a direct and inverse problem. It first considers the physical coupling between melt viscous motion, metal diffusion from the melt toward the fluid phase. The chemical aspects relate to the difference in chemical potential between the three phases that has to re-equilibrate.

The magma reservoir is the place where metal enrichment results from a competition between three different systems, two being basically physical, and a third one chemical. First metals are in the melt and have the choice either to stay in it and latter integrate solid crystals, or to move into the mobile MVP. It basically depends on the chemical attraction of metals between those two phases. Physically, the fate of the metals depends on a competition between diffusion from the melt toward MVP and advection of the melt. The second process, metals diffusion, is intrinsic to metals and magma composition. Third, the melt motion within a tortuous mush of crystals depends on melt viscosity. The three competing processes should be addressed before solving the quantitative aspect of metal enrichment. Because the amount of the three phases varies continuously, the microphysics of the mush-melt-MVP interactions requires a Lagrangian description (Huber et al., 2012; Parmigiani et al., 2014). It provides a qualitative description of the processes. Remains to solve the quantitative problem, that requires a different approach.

5.2.1. The direct problem: Coupling metal partitioning, diffusion, and melt viscosity

A global model has been conceptualized from a lattice Boltzmann model (LBM) simulation to understand the competition between metals diffusion from the melt toward the more mobile immiscible phase and their transport by advection through the mush (Huber et al., 2012). The competition between diffusion and advection points toward assigning a Péclet

number for each couple of magma/metal. A first description assumes a Péclet number equivalent to 10^{-9}/D providing a threshold for metal diffusivity (D) in a felsic magma (Huber et al., 2012). Nevertheless, the model suffers from the large quantitative uncertainties underlying the diffusivity values and the partition coefficients. First elaborated for porphyry-type (Cu, Mo, W, Sn) deposits (Huber et al., 2012; Vigneresse, 2019), the model uses for simplicity a relative enrichment with respect to one component (Cl) of the MVP. It is the most common situation and best documented case of ore deposits related to granitic intrusions (Hedenquist et al., 2005).

The maximum enrichment factor incorporates the Péclet numbers, i.e. the inverse of metal diffusivities and the melt viscosity along the length of the magma reservoir, with a coefficient (c) and a power law (b) coefficient, numerically adjusted (Huber et al., 2012).

$$E_{me\text{-}Cl}|_{max} = (K_{me}/K_{Cl}) \, [1+(c \, Pe_{Cl})^b/(1+(c \, Pe_{me})^b] \qquad (11)$$

The important point of this model is to isolate the controlling interactions between metals, melt and the fluid phase. The metal enrichment factor is bracketed between a minimum value, equivalent to the ratio of metal partitioning between the melt and MVP, and a maximum value. The latter is the preceding minimum value to which terms are added depending on metal diffusion into the melt and melt motion (Vigneresse, 2019). In case of relative enrichment, and for high values of both Péclet numbers (>> 1), the second term of the equation converges toward the ratio of the two Péclet numbers. The second numerical coefficient (c) simplifies to 1. Just remains in the second term of the equation the power law in Péclet number, with the coefficient b, numerically fitted to 1.456 for low Péclet numbers, but to 1.03 for high values corresponding to advection (Huber et al., 2012). The quantification issued from the model indicates an enrichment factor of three orders of magnitude for Au and Cu in porphyry-type magmas (Vigneresse, 2019). The threshold imposed on metal diffusivity

in a felsic melt make Pb and As enrichment unlikely in such magmas. Since it basically consists in a competition between diffusive-like processes, the analytical solution is a suite of exponential functions for metal diffusion in the melt, melt viscous motion and diffusion of chemical potential to reach equilibrium. Keeping this in mind allowed an inverse formulation of the problem (see next section).

The direct approach through LBM (Huber et al., 2012) nicely describes the interactions between each phase. It illustrates the necessary role of a developing mush that slows down melt motion, leaving more time for metal diffusion toward the MVP. Being tapped by the mush, the MVP now enriched in metals, must overcome a threshold before it catastrophically breaks the loose structure of the mush. The overpressure differs from a transition from hydrostatic to lithostatic, as previously suggested (Fournier, 1991; Shinohara and Hedenquist, 1997). It corresponds to a transition from gaseous bubbles to tubes (Parmigiani et al., 2016). Nevertheless, melt decompression would alter the supercriticality of the fluid phase before metals can precipitate.

5.2.2. The inverse problem: Metal enrichment

Building an inverse formulation for ore genesis is not straightful due to the many involved parameters (diffusivity, viscosity, phase amount and composition). The key point is to start from the metal enrichment factor (Eq. 11), determining a relationship with the above-mentioned parameters (Vigneresse, 2019). It indicates that a Péclet number rules the competition between advection and diffusion. Metals partitioning between phases is the other controlling factor. Both have distinct background, physical and chemical, that cannot be simply inverted by a single equation (Lagrangian or Eulerian). The Péclet number must be first expanded, taking into account the viscosity of the melt and the size of the bubbles (Huber et al., 2012). The latter has a restricted effect on the bulk inverse equation, but it fits a

dimensional analysis of the equation. Another possibility is to use the Eyring equation relating diffusivity (D) and viscosity (η) to temperature (Eyring, 1935; Avranov, 2009) following the Stokes-Einstein equation providing the difference in activation energy is small between metal diffusivity and melt viscosity (Mungall, 2002). Such assumption is verified for cations with high activation energy, like high field strength elements (HFSE), i.e. most common metals with high valence. The equation states, using a falling particle of radius r and with B a constant (either 2 or 6π in hydrodynamics), and k the Boltzmann constant, states as

$$D = kT/Br\eta \qquad (12)$$

It results that the product log ($D\eta/T$) is constant at 12.2 providing a rough estimate of log ($D\eta$) at 9 for the temperature of a crystallizing felsic melt (Mungall, 2002; Avranov, 2009). Using this equation, it seems clear that magma viscosity should enter into the inverse equation to be valid for any magma, as well as the size of the bubble. Because the latter is very small compared to other parameters, and does not vary for different magmas, it could be skipped.

It is easy to link the other parameters since they all show an Arrhenian behavior, thus bringing homogeneity in the successive equations. A second point is to consider the large uncertainties on the experimentally measured parameters (diffusion and partitioning). Metal diffusivity in magmas strongly depends on temperature, but this can be handled by fixing it to that of a mush. Dependence on the magma composition; i.e. on its melt structure, is another source of uncertainties, with a range of 1 to 2 orders of magnitude (Zhang et al., 2010). At last, partition coefficients depend on the salt content into the MVP (see review in Vigneresse et al., 2019). The use of a logarithmic scale is a way to smooth the uncertainties on the parameters, taking advantage of their Arrhenian nature.

Partitioning ($K^{melt/MVP}$) represents the return to equilibrium between the chemical potential (μ) of each phase. Consequently, it is preferred to determine partitioning through the usual chemical descriptors of elements (Vigneresse and Truche, 2018). The chemical potential is the equivalent of electronegativity (χ) with a sign changed (Pearson, 1997). The use of electronegativity (usually scaled in eV, equivalent to kJ/mole) is preferred to the usual K values experimentally measured, but presenting a too large spread (Vigneresse, 2019). Metal diffusivity in the melt (D in m^2/s) and viscosity (η in Pa.s) are selected for each pair of melt and magma. The term in length (the bubble size), that keeps dimensionality can be dropped since it does not depend on the melt composition. A logarithmic scale approximates the maximum enrichment value (E) as the respective sum of those parameters:

$$\log_{10} E = - \log_{10} K^{melt/MVP} - \log_{10} \eta - \log_{10} D \qquad (13)$$

Such a simple formula approximates the enrichment factor as a function of the three competing factors within the melt-MVP-mush and metals interactions. A simple synthetic diagram links the three parameters to a specific metal enrichment (Fig. 11).

A note of caution should then be added to the preceding formulation though the given values fit the observations. Obviously, the logarithmic scale (Eq. 13) minimizes the uncertainties on the input parameters, especially diffusivity and partitioning. The computed enrichment factor should be taken as a bulk metal enrichment, providing an order of magnitude rather than an exact number. Nevertheless, this simple equation is verified in two important cases. First, it has been verified for porphyry-type deposits (Cu, Mo, W, Sn) in case of dioritic to granodioritic magmas (Vigneresse et al., 2019). Then it has been extended to ultramafic and alkaline magmas with subsequent Ni, Ti, V ore deposits. A further extension to carbonatites and REE deposits also fits the equation (Vigneresse et al., submitted). In each

case, the couple metal-magma takes place at different temperatures, changing the values of the parameters (diffusion, viscosity, partitioning).

5.2.3. Cyclicity

The competition between diffusion and advection repeats cyclically. Hence, the MVP builds up and escapes the magma reservoir with metals, but a new cycle starts, which is hardly reproducible by usual modeling techniques (Shahabpoor, 2005). The metal enrichment in the MVP can be viewed as the slow charge of a capacitor in classical electrostatics. Conversely, the decharge of the capacitor takes place as the MVP releases its metal content. Using the hydraulic analogy, a capacitor is like a rubber membrane sealed within a pipe through which the flow of water molecules can pass by stretching the membrane. The flow is controlled by its resistance (R). Such stretching effect is like displacing the charges one plate of the capacitor. The amount of stretch is the capacitance (C). It can store energy. The discharge occurs by releasing the stretch on the membrane. Both events are exponentially ruled with a time constant in RC. The analogy could provide insights to the evolution of an ore deposit with time.

6. Discussion on the suggested model

The suggested model is a compromise between a direct formulation using a LBM formalism and an inverse solution based on metal enrichment. The inverse approach is, at our present knowledge, the first and certainly preliminary, approach to ore genesis.

6.1. Generation of different metallic veins in a given deposit

The direct method would allow to estimate the differential enrichment in metals (Cu, but also Au, Ag, …) observed in most porphyry deposits, just by varying the second order parameters controlling metal diffusivity and magma viscosity. Indeed, a small variation in temperature may alter the metal content within the MVP, thus varying the enrichment and consequently the ore grade. The activation energy for magma viscosity being larger that the one for metal diffusivity, an increase in temperature due to hotter (e.g. mafic) magma should enhance metal enrichment.

Conversely, the inverse approach should give insights to the role of fluids within the MVP. Considering the eq. 13, the value of metal partitioning could be computed, assuming a differential metal enrichment value, whatever its origin. The variation directly correlates with the chemical character of the MVP. Adding S species decreases the electronegativity (i.e. increases its chemical potential), whereas halogens increase electronegativity. The variation in both senses may reach about 1-2 eV, thus resulting in a similar change but in 1-2 order orders of magnitude for the chemical potential difference with the melt.

Such variations in ore grade from vein to vein should find explanation by the different bulk diffusivity values under a given temperature.

6.2.Modeling and exploration

A point that frequently comes out from the reviewers on papers about ore deposits relates to "*how does this paper help me to discover new deposits during exploration ?*" Answering such question is : it does not help. Indeed, there is a basic difference between modeling, that aims to understand processes,and exploration leading to the discovery of new deposits.

The dichotomy between explanatory and predictive modeling reflects the distinct scientific goals, between causal explanation and empirical prediction (Shmueli, 2010). Both use data for explaining or predicting, respectively. In contrast, modeling aims understanding the causal processes. Once those have been identified, then statistical analyses or consequences observable on the field can be used for prediction and exploration. In a different approach, descriptive modeling summarizes the available data and tries identifying their causes. Nevertheless, it is also not aimed at prediction (Sainani, 2014). One basic difference between the two approaches relies on the difference between a quantitative and predictive approach in one hand, and a qualitative approach, commonly more explicative and certainly offering a better understanding of the processes (Thom, 2009). The latter book, written by the Medal Field mathematician who conceptualized the catastrophe theory, also makes the difference between the two approaches.

7. Conclusions

A brief review of models of ore generation within an intrusive context considers the direct, inverse and iterative problems. In the direct problem, starting from given and fixed parameters, a unique solution is proposed, because of its intrinsic over-determination. It denotes a causal relation to the provided solution. By evidence, the resulting model nearly always fits observations, but there is no control on some un-observed feedback loop or complex coupling between variables. The direct approach is widely proposed in the literature of economic geology. Conversely, the inverse problem starts from the measurements, trying to identify the controlling parameters. The solution is non-unique and must satisfy a statistical test on errors, the most used being a least squares norm. Owing to its underlying physical formalism, it is mainly used for the interpretation of geophysical prospections. Finally,

iterative approaches often result in identifying attractors that control a cyclic behavior of the system. From such approaches, a global model has been constructed, extending a previous formulation, valid for porphyry-type deposits and associated metals (Cu, Mo, Au, Ag). Metal enrichment results during the magmatic stage, in a competition between diffusion, i.e. transport within the melt, and advection, i.e. transport by the magmatic volatile immiscible phase. Melt motion, through viscosity and mush formation, through crystallization, also compete together. They constitute the physical aspects of the model. At this competition, another one exists, between metal partitioning between the melt, crystals, and fluid phase. It constitutes the chemical aspects of the competition. Such formalism points to a direct problem, providing metal enrichment factors using a predefinite Péclet number for each metal. Another important principle is to consider the bulk enrichment factor in metals, not necessarily through a precise number, as suggested in the direct method, but using an inverse formalism based on a logarithmic scale. Looking at the order of magnitude, up to five, of the enrichment appears sufficient, contrasting with previous models that hardly reach two orders of magnitude.

Acknowledgments

The paper resulted from a long practice in direct and inverse methods, aimed to delineate the shape at depth of many intrusions. However, modeling rapidly appeared as a topic of study by itself, leading to find a solution with one more decimal than the preceding one. Problems come when the error bar on solutions are less than those on observables. The manuscript benefited from numerous comments and encouragements from the editorial board. They are warmly acknowledged.

References

Ague, J.J., Brimhall, G. 1989. Geochemical modeling of steady state fluid flow and chemical reaction during supergene enrichment of porphyry copper deposits. *Economic Geology,* **84**, 506-526.

Alter, O., Golub, G.H., 2004. Integrative analysis of genome-scale data by using pseudoinverse projection predicts novel correlation between DNA replication and RNA transcription. *PNAS* **101**, 16577-16582.

Améglio, L., Vigneresse, J.L., Bouchez, J.L., 1997. An assessment of combined fabrics and gravity data in granites. In: Bouchez, J.L., Hutton, D., Stephens, W.E. (Eds), *Granite: from melt segregation to emplacement fabrics*. Kluwer Academic Publisher, Dordrecht, 199-214.

Andrews, H., Patterson, H., 1976. Singular value decomposition (SVD) image coding. *IEEE Transactions on Communications* **24**, 426-432.

Animali, S., Karlin, I.V., 2002. Kinetic boundary conditions in the lattice Boltzmann method. *Physical Review* **E66**, 026311.

Annen, C., 2009. From plutons to magma reservoirs: Thermal constraints on the accumulation of eruptible silicic magma in the upper crust. *Earth and Planetary Science Letters* **284**, 409-416.

Arditi, R., Ginzburg, L.R., 2012. *How Species Interact: Altering the Standard View on Trophic Ecology*. Oxford University Press, Oxford, 192 pp.

Arfken, G. 1985. The method of steepest descent. In: *Mathematical Methods for Physicists*. Academic Press, Orlando, pp. 428-436.

Atlan, H., 2011. *Qu'est-ce qu'un modèle ?* Editions Manucius, Paris, 48 pp.

Avranov, I., 2009. Relationship between diffusion, self-diffusion and viscosity. *Journal of Non-Crystalline Solids* **355***,* 745-747.

Backus, G., Gilbert, F., 1970. Uniqueness in the inversion of inaccurate gross Earth data. *Philosophical Transactions of the Royal Society of London* **266**, 123-192.

Barnes, S.J., Lightfoot, P.C., 2005. Formation of magmatic nickel-sulfide ore deposits and processes affecting their copper and platinum-group element contents. *Economic Geology 100th Anniversary Volume*, Society of Economic Geologists 179-213.

Benini, O., Cervellati, R., Fetto, P., 1996. The BZ reaction: Experimental and model studies in the physical chemistry laboratory. *Journal of Chemical Education* **73**, 865-868.

Ben-Israel, A., Greville, T.N.E., 1974. *Generalized Inverses, Theory and Applications.* John Wiley and Sons, London, 410 pp.

Blundy, J., Wood, B.J., 2003. Partitioning of trace elements between crystals and melts. *Earth and Planetary Science Letters* **210**, 383–397

Boudreau, B.P., 1996. The diffusive tortuosity of fine-grained unlithified sediments. *Geochimica et Cosmochimica Acta* **60**, 3139-3142.

Brassinnes, S., Balaganskaya, E., Demaiffe, D., 2005. Magmatic evolution of the differentiated ultramafic, alkaline and carbonatite intrusion of Vuoriyarvi (Kola Peninsula, Russia). A LA-ICP-MS study of apatite. *Lithos* **85**, 76-92.

Breiter, J., Förster, H.J., Seltmann, R., 1999. Variscan silicic magmatism and related tin-tungsten mineralization in the Erzgebirge-Slavkovský les metallogenic province. *Mineralium Deposita* **34**, 505-521.

Burg, J.P., Vigneresse, J.L., 2002. Non-linear feedback loops in the rheology of cooling-crystallizing felsic magma and heating-melting felsic rock. *Geological Society, London, Special Publications* 200, 275-292.

Burks, A.W., 1970. Von Neumann's self-reproducing automata. In: Burks, A.W. (Ed), *Essays on Cellular Automata*, University of Illinois Press, 3-64.

Campos, E.A., Wijbrans, J., Andriensen P.A.M., 2009. New thermochronologic constraints on the evolution of the Zaldívar porphyry copper deposit, Northern Chile. *Mineralium Deposita* **44**, 329-342.

Castro, A., Moreno-Ventas, I., De La Rosa, J.D., 1991. H-type (hybrid) granitoids: A proposed revision of the granite-type classification and nomenclature. *Earth Science Reviews* **31**, 237-253.

Cathles, L.M., Adams, J.J., 2005. Fluid flow and petroleum and mineral resources in the upper (< 20 km) continental crust. *Economic Geology 100th Anniversary Volume*. Society of Economic Geologists 77-110.

Chelle-Michou, C., Rottier, B., Caricchi, L., Simpson, G., 2017. Tempo of magma degassing and the genesis of porphyry copper deposits: *Nature Scientific Reports* **7**, doi: 10.1038/srep40566

Chi, G., Xue, C., 2011. An overview of hydrodynamic studies of mineralization. *Geoscience Frontiers* **2**, 423-438.

Chopard, B., Droz, M., 1998. *Cellular Automata Modeling of Physical Systems.* Cambridge University Press, 342 pp.

Cousins, C.A., 1959. The structure of the mafic portion of the Bushveld Igneous Complex. *South African Journal of Geology* **62**, 179-201.

Delgado, J., Hernández-Martínez, L.I., Pérez-López, J., 2017. Global bifurcation map of the homogeneous states in the Gray-Scott model. *International Journal of Bifurcation and Chaos* **27**, 1730024, doi /10.1142/S0218127417300245.

Dolgal, A.S., Balk, P.I., Novikova, P.N., Michurin, A.V., 2016. Matching criteria of acceptable solutions for gravity ore type inverse problem. *Geophysical Research* **17**, 17-31.

Edmonds, M., Woods, A.W., 2018. Exsolved volatiles in magma reservoirs. *Journal of Volcanology and Geothermal Research* **308**, 13-30.

Eppelbaum, L.V., 2014. Application of potential geophysical fields in ore deposits: Inverse problem solution under complex conditions and 3D gravity-magnetic field modeling. *Proceedings of the 2014 SAGEEP Conference* **27**, 359-368.

Eyring, H., 1935. The activated complex in chemical reactions. *Journal of Chemical Physics,* 107–115.

Fernández-Martínez, J.L., 2015. Model reduction and uncertainty analysis in inverse problems. *The Leading Edge* **34**, 1006-1016.

Fournier, R. O., 1991. Transition from hydrostatic to greater than hydrostatic fluid pressure in presently active hydrothermal systems in crystalline rocks. *Geophysical Research Letters* **18**, 955-958.

Franklin, J.N., 1970. Well-posed stochastic extensions of ill-posed linear problems. *Journal of Mathematical Analysis* **31**, 682-716..

Fu, F.Q., McInnes, B.I.A., Evans, N.J., Davies, P.J., 2010. Numerical modeling of magmatic–hydrothermal systems constrained by U–Th–Pb–He time–temperature histories. *Journal of Geochemical Exploration* **106**, 90-109.

Garven, G., 1995. Continental scale groundwater flow and geological processes. *Annual Review of Earth and Planetary Processes* **23**, 89-117.

Ghasemzadeh-Barvarz, M., Beaudoin, G., Grunsky, E.C., McClenaghan, M.B., Duchesne, C., Boutroy, E., 2016. Partial least squares-discriminant analysis of trace element compositions of magnetite from various VMS deposit subtypes: Application to mineral exploration. *Ore Geology Reviews* **78**, 388-408.

Gilbert, F., 1971. Ranking and winnowing gross Earth data for inversion and resolution. *Geophysical Journal of the Royal Astronomical Society* **23**, 125-128.

Glendinning, P., 1995. *Stability, Instability and Chaos. An Introduction to the Theory of Nonlinear Differential Equations*. Cambridge University Press, 404 pp.

Golub, G.H., Reinsch, C., 1970. Singular value decomposition and least squares solutions. *Numerische Mathematik* **14**, 403-420.

Gray, P., Scott, S., 1990. *Chemical Oscillations and Instabilities*. Oxford University Press, Oxford, 469 pp.

Guillou-Frottier, L., Burov, E.B., 2003. The development and fracturing of plutonic apexes: Implications for porphyry ore deposits. *Earth and Planetary Sciences Letters* **214**, 341-356.

Hale, J.K., Peletier, L.A., Troy, W.C., 1999. Stability and instability in the Gray-Scott model. The case of equal diffusivities. *Applied Mathematics Letters* **12**, 59-65.

Hedenquist, J.W., Seedorff, E., Thompson, J.F.H., Dilles, J.H., Goldfarb, R.J., Proffett, J.M.Jr., Richards, J.P., Einaudi, M.T., Zurcher, L, Stavast, W.J.A., Johnson, D.A., Barton, M.D., 2005. Porphyry deposits: Characteristics and origin of hypogene features. *Economic Geology, 100th Anniversary Volume*, Society of Economic Geologists, 251-298.

Herrmann, W., Berry, R.F., 2002. MINSQ – a least squares spreadsheet method for calculating mineral proportions from whole rock major element analyses. *Geochemistry: Exploration, Environment, Analysis* **2**, 361-368.

Hildreth, W., Moorbath, S., 1998. Crustal contributions to arc magmatism in the Andes of central Chile. *Contributions to Mineralogy and Petrology* **98**, 455-489.

Holling, C.S., 1973. Resilience and stability of ecological systems. *Annual Review of Ecology and Systematics* **4,** 1-23.

Howard, A., 1984. *Elementary Linear Algebra.* Wiley, New York, 464 pp.

Huber, C., Bachmann, O., Vigneresse, J.L., Dufek, J., Parmigiani, A., 2012. A physical model for metal extraction and transport in shallow magmatic systems. *Geochemistry, Geophysics, Geosystems* **12**, doi:10.1029/2012GC004042.

Huber, C., Parmigiani, A., Chopard, B., Manga, M., Bachmann, O., 2008. Lattice Boltzmann model for melting with natural convection. *International Journal of heat and Fluid Flow* **29**, 1469-1480.

Iacopini, D., Carosi, R., Xypolias, P., 2010. Implications of complex eigenvalues in homogeneous flow: A three-dimensional kinematic analysis. *Journal of Structural Geology* **32**, 93-106.

Jackson, D.D., 1972. Interpretation of inaccurate, insufficient and inconsistent data. *Geophysical Journal of the Royal Astronomical* Society **28**, 97-100.

Ju, M., Yang, J., 2011. Numerical modeling of coupled fluid flow, heat transport and mechanical deformation: An example from the Chanziping ore district, South China. *Geoscience Frontiers* **2**, 577-582.

Kang, Q., Zhang, D., Chen, S., He, X., 2006. Lattice Boltzmann simulation of chemical dissolution in porous media. *Physical Review* **E65**, 036318, doi 10.1103/PhysRevE.65.036318

Kelka, U., Veveakis, M., Koehn, D., Beaudoin, N., 2017. Zebra rocks: compaction waves create ore deposits. *Scientific Reports* **7**, 14260**.**

Kelley, K.D., Scott, C.T., Polyak, D.E., Kimball, B.E., 2017, Vanadium. chap. U of Schulz, K.J., DeYoung, J.H., Jr., Seal, R.R., II, and Bradley, D.C., (eds.). *Critical Mineral Resources of the United States—Economic and Environmental Geology and Prospects for Future Supply*. USGS Professional Paper **1802**, U1-U36.

Kemp, A.I.S., Hawkesworth, C.J., Foster, G.L., Paterson, B.A., Woodhead, J.D., Hergt, J.M., Gray, C.M., Whitehouse, M.J., 2007. Magmatic and crustal differentiation history of granitic rocks from Hf-O isotopes in zircon. *Science* **315**, 980-983.

Kinnaird, J.A., Kruger, F.J., Nex, P.A.M., Cawthorn, R.G., 2002. Chromitite formation - a key to understanding processes of platinum enrichment. *Transaction of the Institute of Mining and Metallurgy* **111**, B23-B35.

Klein, C., 2005. Some Precambrian banded iron-formations (BIFs) from around the world: Their age, geologic setting, mineralogy, metamorphism, geochemistry, and origin. *American Mineralogist* **90**, 1473-1499.

Kolmogorov, A., 1931. Über die analytischen Methoden in der Wahrscheinlichkeitsrechnung. *Mathematische Annalen* **104**, 415-458.

Krneta, S., Ciobanu, C.L., Nigel, N J. Cook, N.J., Ehrig, K.J., 2018. Numerical modeling of REE fractionation patterns in fluorapatite from the Olympic Dam deposit (South Australia). *Minerals* **8**, 342-362.

Kun, W., Keyan, X., Nan, L., Yuan, C., Shengmiao, L., 1987. Robust statistics and geochemical data analysis. *Mathematical Geology* **19**, 207-218.

L'Heureux, I., 2013. Self-organized rhythmic patterns in geochemical systems. *Philosophical Transactions of the Royal Society of London* **A371**, 20120356, doi /10.1098/rsta.2012.0356.

Landtwing, M.R., Dillenbeck, E.D., Leake, M.H., Heinrich, C.A., 2002. Evolution of the breccias-hosted porphyry Cu-Mo-Au deposit at Agua Rica, Argentina: Progressive unroofing of a magmatic hydrothermal system. *Economic Geology* **97**, 1273-1292.

Landtwing, M.R., Furrer, C., Redmond, P.B., Pettke, T., Guillong, M., Heinrich, C.A., 2010. The Bingham Canyon porphyry Cu-Mo-Au deposit. III. Zoned copper-gold ore deposition by magmatic vapor expansion. *Economic Geology* **105**, 91-118.

Lawson, C.L., Hanson, R.J., 1987. *Solving Least Squares Problems*. Society for Industrial and Applied Mathematics, 369 pp.

Lee, C.T.A., Lee, T.C., Wu, C.T., 2014. Modeling the compositional evolution of recharging, evacuating, and fractionating (REFC) magma reservoirs: Implications for differentiation of arc magma. *Geochimica et Cosmochimica Acta* **143**, 8-22.

Lerchbaumer, L., Audétat, A., 2013. The metal content of silicate melts and aqueous fluids in subeconomically Mo mineralized granites: Implications for porphyry Mo genesis. *Economic Geology* **108**, 987-1013.

Liu, L.M., Yang, G.Y, Peng, S.L., Zhao, C. 2008. Numerical modeling of coupled geodynamical processes and its role in facilitating predictive ore discovery: An example from Tongling, China. *Resource Geology* **55**, 21-31.

Lotka, A.J., 1910. Contribution to the theory of periodic reaction. *Journal of Physical Chemistry* **14**, 271-274.

Maier, W.D., Groves, D.I., 2011. Temporal and spatial controls on the formation of magmatic PGE and Ni–Cu deposits. *Mineralium Deposita* **46**, 841-857.

Malehmir, A., Bellefleur, G., 2009. 3D seismic reflection imaging of volcanic-hosted massive sulfide deposits: Insights from reprocessing Halfmile Lake data, New Brunswick, Canada. *Geophysics* **74**, B209-B219.

Manneville, P., 1991. *Structures Dissipatives, Chaos et Turbulence*. Arléa, Saclay, 420 pp.

Marconi, S., Chopard, B., 2003. A lattice Boltzmann model for a solid body. *International Journal of Modern Physics* **B17**, 153-156.

Marquardt, D.W., 1963. An algorithm for least-squares estimation of nonlinear parameters. *Journal of the Society for Industrial and Applied Mathematics* **22**, 431-441.

McKenzie, D., 1984. The generation and compaction of partially molten rocks. *Journal of Petrology* **25**, 713-765.

Meinhardt, H., 2009. *The Algorithmic Beauty of Sea Shells*. Springer, Heidelberg, 269 pp.

Melnik, O., Bindeman, I., 2018. Modeling of trace elemental zoning patterns in accessory minerals with emphasis on the origin of micrometer-scale oscillatory zoning in zircon. *American Mineralogist* **103**, 353-368.

Mitchell, R.H., 2005. Carbonatites and carbonatites and carbonatites. *The Canadian Mineralogist* **43**, 2049-2068.

Mouhers, M.E., 2015. *Numerical modelling study on the quantification of in-situ leaching (ISL) of copper in porphyry rock*. Thesis Faculty of Geosciences, Utrecht University, 94 pp.

Mungall, J.E., 2002. Empirical models relating viscosity and tracer diffusion in magmatic silicate melts. *Geochimica et Cosmochimica Acta* **66**, 125-143.

Murray, J.D., 1993. *Mathematical Biology*. Springer, Heidelberg, 553 pp.

Myagkiy, A., Truche, L., Cathelineau, M., Golfier, F., 2017. Revealing the conditions of Ni mineralization in the laterite profiles of New Caledonia: insights from reactive geochemical transport modelling. *Chemical Geology* **466**,274-284.

Nadeau, O., Stix, J., Williams-Jones, A.E., 2013. The behavior of Cu, Zn and Pb during magmatic–hydrothermal activity at Merapi volcano, Indonesia. *Chemical Geology* **342**, 167-179.

Nicolis, G., Prigogine, A., 1977. *Self-Organization in Nonequilibrium Systems*. John Wiley and Sons, 490 pp.

O'Brien, G.S., Bean, C.J., McDermott, F., 2003. Numerical investigations of passive and reactive flow through generic single fractures with heterogeneous permeability. *Earth and Planetary Science Letters* **213**, 271-284.

Oberst, S., Niven, R.K., Lester, D.R., Ord, A., Hobbs, B., Hoffmann, N., 2018. Detection of unstable periodic orbits in mineralizing geological systems. *Chaos* **28**, 085711.

Ortoleva, P., 1994. *Geochemical Self-Organization*. Oxford University Press, 426 pp.

Parker, R.L.., 1970. The inverse problem of electrical conductivity in the mantle. *Geophysical Journal of the Royal Astronomical Society* **22**, 121-138.

Parmigiani, A., Faroughi, S., Huber, C., Bachmann, O., Su, Y., 2016. Bubble accumulation and its role in the evolution of magma reservoirs in the upper crust. *Nature* **532**, 492-495.

Parmigiani, A., Huber, C., Bachmann, 2014. Mush microphysics and the reactivation of crystal-rich magma reservoirs. *Journal of Geophysical Research* **B119**, 6308-6322.

Pazdiniakou, A., Tinet, A.J., Golfier, F., Kalo, K., Gaboreau, S., Gaire, P., 2018. Numerical efficiency of the lattice Boltzmann model for digital nano-porous rock applications. *Advances in Water Resources* **121**, 44-66.

Pearson, R.G., 1997. *Chemical Hardness*. John Wiley and Sons, New York, 210 pp .

Petrascheck, W.E., 1965. Typical features of metallogenic provinces. *Economic Geology* **60**, 1620-1634.

Pokrovski, G.S., Borisova, A.Y., Harrichoury, J.C., 2008. The effect of sulfur on vapour-liquid fractionation of metals in hydrothermal systems. *Earth and Planetary Science Letters* **266**, 345-362.

Prigogine, I., 1978. Time, structure, and fluctuations. *Science* **201**, 4358, 777-785.

Rabinowicz, M., Vigneresse, J.L., 2004. Melt segregation under compaction and shear channelling: Application to granitic magma segregation in a continental crust. *Journal of Geophysical Research* **B109**, 10.1029/2002JB002372.

Robb, L., 2005. *Introduction to Ore-forming Processes*. Blackwell Publishing Company, 373 pp.

Sadek, R.A., 2012. Based image processing applications: State of the art, contributions and research challenges. *International Journal of Advanced Computer Science and Applications* **3**, 26-34.

*Sahidullah, M., Kinnunen, T., 2016. Local spectral variability features for speaker verification. Digital Signal Processing **50**, 1-11.*

Sainani, K.L., 2014. Explanatory versus predictive modeling. *PM&R* **6**, 841-844.

Schöpa, A., Annen, C., 2013. The effects of magma flux variations on the formation and lifetime of large silicic magma reservoirs. *Journal of Geophysical Research* **B118**, 926-942.

Schöpa, A., Annen, C., Dilles, J.H., Blundy, J.D., Sparks, S., 2017. Magma emplacement rates and porphyry copper deposits. Thermal modeling of the Yerington Batholith, Nevada. *Economic Geology* **112**, 1653-1672.

Seo, J.H., Guillong, M., Heinrich, C.A., 2009. The role of sulfur in the formation of magmatic–hydrothermal copper–gold deposits. *Earth and Planetary Science Letters* **282**, 323-328.

Shahabpour, J., 2010. Feedback concepts in the ore-forming systems. *Resource Geology* **60**, 109-115.

Shan, X., Yuan, X.F., Chen, H., 2006. Kinetic theory representation of hydrodynamics: A way beyond the Navier-Stokes equation. *Journal of Fluid Dynamics* **550**, 413-441.

Shinohara, H., Hedenquist, J. W., 1997. Constraints on magma degassing beneath the Far Southeast Porphyry Cu–Au deposit, Philippines. *Journal of Petrology* **38**, 1741-1752.

Shmueli, G., 2010. To explain or to predict? *Statistical Science* **25**, 280-310.

Sillitoe, R.H., 2010. Porphyry copper systems. *Economic Geology* **105**, 3-41.

Sinclair, W.D., 2007. Porphyry deposits. In: Goodfellow, W.D., (Ed.), *Mineral Deposits of Canada: A Synthesis of Major Deposit-Types, District Metallogeny, the Evolution of*

Geological Provinces, and Exploration Methods. Geological Association of Canada, Mineral Deposits Division, Special Publication, Canada, Newfoundland, 223-243.

Steefel, C.I., Lichtner P.C., 1994. Diffusion and reaction in rock matrix bordering a hyperalkaline fluid-filled fracture**.** *Geochimica et Cosmochimica Acta* 58, 3595-3612.

Štemprok, M., 1982. Tin-fluorine-relationships-in-ore-bearing-assemblages. In *Metallization Associated with Acid Magmatism*., A.M. Evans (Ed.) Wiley & Sons, 321-337.

Suga, S., 2006. Numerical schemes obtained from lattice Boltzmann equations for advection diffusion equations. *International Journal of Modern Physics* **C17**, 1563-1577.

Süli, E., Mayers, D., 2003. *An Introduction to Numerical Analysis*. Cambridge University Press, 444 pp.

Talwani, M., Worzel, J.L., Landisman, M., 1959. Rapid gravity computations for two-dimensional bodies with application to the Mendocino submarine fracture zone. *Journal of Geophysical Research* **64**, 49-59.

Tarantola, A., 2005. *Inverse Problem Theory and Methods for Model Parameter Estimation*. Society for Industrial & Applied Mathematics, 352 pp.

Tarantola, A., 2006. Popper, Bayes and the inverse problem. *Nature Physics* **2**, 492-494.

Tauson, V.L., Lipko, S.V., Smagunov, N.V., Kravtsova, R.G., 2018. Trace element partitioning dualism under mineral–fluid interaction: Origin and geochemical significance. *Minerals* **8**, 282, doi 10.3390/min8070282

Teschl, G., 2012. *Ordinary Differential Equations and Dynamical Systems*. American Mathematical Society**, 356 pp.**

Thom, R., 2009. *Prédire n'est pas expliquer.* Flammarion, Paris, 171 pp.

Toffoli, T., Margolus, N., 1987. *Cellular Automata Machines: A New Environment for Modeling*. The MIT Press, 259 pp.

Trefethen, L.T., Bau, III D., 1997. *Numerical Linear Algebra*. Society for Industrial and Applied Mathematics, 187 pp.

Turing, A.M., 1937. On computable numbers with an application to the Entscheidungsproblem. *Proceedings of the London Mathematical Society* 2, **42**, 230–65.

Vigneresse, J.L., 1977. Linear inverse problem in gravity profile interpretation. *Journal of Geophysics* **43**, 193-213.

Vigneresse, J.L., 1978. Damped and constrained least squares method with application to gravity interpretation. *Journal of Geophysics* **45**, 17-28.

Vigneresse, J.L., 1990. Use and misuse of geophysical data to determine the shape at depth of granitic intrusions. *Geological Journal* **25**, 249-260.

Vigneresse, J.L., 1999. Should felsic magmas be considered as tectonic objects, just like faults or folds? *Journal of Structural Geology* **21**, 11251-130.

Vigneresse, J.L., 2008. Granitic batholiths: from pervasive and continuous melting in the in the lower crust to discontinuous and spaced plutonism in the upper crust. *Transactions of the Royal Society of Edinburgh: Earth Sciences* **97**, 311-324.

Vigneresse, J.L., 2015. Textures and melt-crystal-gas interactions in granites. *Geoscience Frontiers* **6**, 635-663

Vigneresse, J.L., 2019. Addressing ore formation and exploration. *Geoscience Frontiers* **10**, 1613-1622.

Vigneresse, J.L., Barbey, P., Cuney, M., 1996. Rheological transitions during partial melting and crystallization with application to felsic magma segregation and transfer. *Journal of Petrology* **37**, 1597-1600.

Vigneresse, J.L., Burg, J.P., 2000. Continuous vs. discontinuous melt segregation in migmatites: insights from a cellular automaton model. *Terra Nova* **12**, 188-192.

Vigneresse, J.L., Burg, J.P., 2006. Simulation of crustal melt segregation through cellular automata: Insight on steady and non-steady state effects under deformation. *Pure and Applied Geophysics* **162**, 987-1011.

Vigneresse, J.L., Richard, A., Truche, L., 2019. A tentative conceptual and quantitative model for metal enrichment in silicate and carbonatite magmas with applications to ore deposits. *Ore Geology Reviews* (submitted)

Vigneresse, J.L., Truche, L., 2018. Chemical descriptors for describing physico-chemical properties with applications to geosciences. *Journal of Molecular Modeling* **24**, 231, doi s00894-018-3770-0

Vigneresse, J.L., Truche, L., Richard, A., 2019. How do metals escape from magmas to form porphyry-type ore deposits? *Ore Geology Reviews* **105**, 310-336.

Volterra, V., 1926. Variazioni e fluttuazioni del numero d'individui in specie animali conviventi. *Memoria Accademia dei Lincei Roma* **2**, 31-113.

Weis, P., Driesner, T., Heinrich, C.A., 2012. Porphyry-copper ore shells form at stable pressure-temperature fronts within dynamic fluid plumes. *Science* **338**, 1613-1616.

Wiggins, R.A., 1972. The general linear inverse problem. Implication of surface waves and free oscillations for Earth structure. *Reviews of Geophysics and Space Physics* **10**, 251-285.

Wilkinson, J., 2001. Fluid inclusions in hydrothermal ore deposits. *Lithos* **55**, 229-272.

Wolfram, S., 1983. Statistical mechanics of cellular automata. *Reviews of Modern Physics* **56**, 601-645.

Wright, C.J., McCarthy, T.S., Cawthorn, R.G., 1983. Numerical modelling of trace element fractionation during diffusion controlled crystallization. *Computers and Geosciences* **9**, 368-389.

Xypolias, P., 2010. Vorticity analysis in shear zones: A review of methods and applications. *Journal of Structural Geology* **32**, 2072-2092.

Yu, C., 1988. Ore-forming processes and dissipative structures. *Acta Geologica Sinica* **1**, 177-192.

Zaitsev, A., Bell, K., 1995. Sr and Nd isotope data of apatite, calcite and dolomite as indicators of source, and the relationships of phoscorites and carbonatites from the Kovdor massif, Kola peninsula, Russia. *Contributions to Mineralogy and Petrology* **121**, 324-335.

Zajacz, Z., Halter, W.E., Pettke, T., Guillong, M., 2008. Determination of fluid/melt partition coefficients by LA-ICPMS analysis of co-existing fluid and silicate melt inclusions: Controls on element partitioning. *Geochimica et Cosmochimica Acta* **72**, 2169-2197.

Zelenski, M., Bortnikova, S., 2005. Sublimate speciation at Mutnovsky volcano, Kamchatka. *European Journal of Mineralogy* **17**, 107-118.

Zhang, Y., Ni, H., Chen, Y., 2010. Diffusion data in silicate melts. *Reviews in Mineralogy and Geochemistry* **72**, 311-408.

Zhang, Y., Robinson, J., Schaubs, P.M., 2011. Numerical modelling of structural controls on fluid flow and mineralization. *Geoscience Frontiers* **2**, 449-461.

Zhao, C., Reid, L.B., Regenauer-Lieb, K., 2014. Some fundamental issues in computational hydrodynamics of mineralization: A review. *Journal of Geochemical Exploration* **112**, 21-34.

Figure captions

Figure 1. Ore grade (g/t) as a function of ore tonnage (Mtons). Data sets for Cu, Mo, W, Au are redrawn from Sinclair (2007), and data for V and REE are from Kelley et al., (2017). The major idea coming out from this diagram is the global grade ranging 0.1 to 10 %, that slightly increases for Ni and PGE, thus increasing the enrichment factor (E), owing to the lower initial abundance in such metals (see Fig. 2).

Figure 2. Abundance of elements as a function of 10^6 atoms of Si. Elements are in their atomic number (Z) order, and are grouped as lithophile and siderophile elements. Rare earth elements (REE) are individualized, as well as platinum group elements (PGE). The relative abundance of most metals ranges 10^{-5} to 10^2 relative to Si, that is 10^{-11} to 10^{-4} in absolute values.

Figure 3. Illustration of the direct, inverse and iterative problem in the case of ore deposit formation. In the direct problem, the inputs are the parameters of the melt, metals and MVP that are thought to control magma reservoir evolution and metal enrichment (E). The solution is unique, but strongly dependent on the causal parameters that are fixed. In the inverse problem, the parameters are deduced from the model, leading to several solutions, that should be separated using a statistical test on the errors. In the iterative problem, an initial model is built, and the parameters are further refined to match the enrichment.

Figure 4. Eulerian versus Lagrangian approaches to a flux of matter. The former approach considers an external reference frame. The rate of change with time of some fluid property ($\partial/\partial t$) generally includes a term accounting for convection. Conversely, in the Lagrangian approach, the frame is attached to a particle. D/Dt represents the acceleration of an individual element as it speeds up or slows down during its motion.

Figure 5. Lattice Boltzmann Model illustrated by the interactions between adjacent particles, in 2D (plan) and 3D (volume). The result is the coding of each particle as a function of its content, e.g. melt or MVP. Picture of the model during computation adapted from the modeling by A. Parmigiani (Huber et al., 2012) showing the gas phase within the mush (in light grey).

Figure 6. Matrix problem ($\mathbf{m} = \mathbf{A}\,\mathbf{x}$), full, under-, and over-determined problem, with the unscaled matrix spectrum Sp($\mathbf{A}$), a plot of the eigenvalues in decreasing amplitude. The values close to nullity should be removed, indicating redundant and un-significant solutions, thus un-significant equations. The characteristics of the matrix, such as the trace Tr($\mathbf{A}$), its determinant det($\mathbf{A}$) and its conditions number $\kappa(\mathbf{A})$ are indicated, all resulting from the eigen-equation. The colors used to represent the vectors and the subsequent matrix components have no significance in terms of amplitude or values. This is also valid in the successive illustrations about matrix computation.

Figure 7. Rotational and scaling aspects of the singular value decomposition starting from a unit disc with the initial geometric coordinates (X and Y). The eigenvectors (σ_1 and σ_2) of matrix **A** are successively rotated through matrix $\mathbf{V^T}$ and **U** and scaled through the matrix **S**. The successive rotations and scaling modify the position of the original coordinates into a new coordinates system (σ_1 and σ_2) transforming the unit disc into an ellipse. Hence the columns of U are eigenvectors of eigenvectors of $\mathbf{A^TA}$ and the columns of **V** are eigenvectors of $\mathbf{AA^T}$. They form a new orthonormal basis for the system.

Figure 8. Singular value decomposition. The matrix **A** is rotated and scaled (Fig. 7) through the matrix **U** and **V**. It finally results in a matrix **S**, pseudo eigenmatrix of the system. The respective products $\mathbf{U\,U^T}$ and $\mathbf{V\,V^T}$ are the unity matrix **I**, with only diagonal terms equal to 1. Conversely the columns of U and V form a new orthonormal basis for the system, according to the successive rotations and scalings.

Figure 9. Map of different types of 2D flow in a referential constructed from Tr(**A**) and det(**A**). The former discriminates between sources and sinks, whereas det(**A**) separates the field of pure to simple shear. A parabola considers the degenerate solutions. A simple inspection on the eigen characters of the matrix immediately provides the type of flow it induces. Such diagrams are of great interest in understanding ductile deformation, pertaining to viscous flow regimes.

Figure 10. Model of fluid sparging in case of porphyry-type deposits. The magma reservoir is represented with no crystals, a yet abundant mush, and a tapping mush. The MVP exsolves from a periodically replenished magma reservoir. The new magma is rapidly assimilated since the magma reservoir is buffered in oxygen, and sulphur. Metals represented as small plain drops diffuse into the melt, and preferentially incorporate the immiscible phase. They first form bubbles, that progressively turn to tubes when they accumulate in the mush. The equivalent diagram representing the Péclet (advection/diffusion) and Stefan (sensible heat/latent heat) numbers shows this transition from bubbles to tubes. When the mush is too stiff to resist the MVP buoyancy, the latter escapes through high strain rate, switching from lithostatic and supercritical to a simple hydrostatic regime. Metals precipitate while MVP alters the surroundings. The process is cyclic, induced by magma replenishment.

Figure 11. Global enrichment in case of Cu-Au porphyry deposits. The diagram is scaled in temperature between 600 and 700 °C, versus the parameters (diffusion D, viscosity η and partitioning K) in a logarithmic scale. The sum of those parameters (Eq. 12) provides the enrichment factor (E), as indicated by the arrows. The case of Cu is illustrated within a felsic magma, as it develops in porphyry type deposits. The enrichment must then be corrected by the initial metal abundance to reach ore grade.

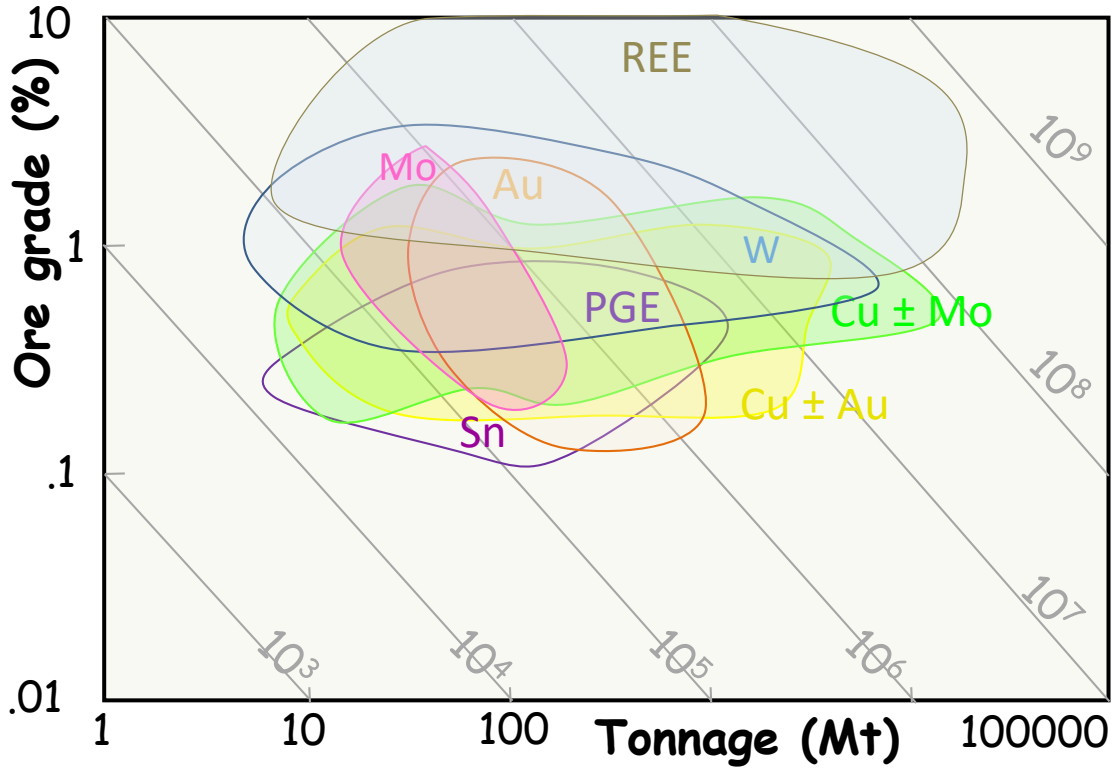

Vigneresse & Truche

Fig. 1

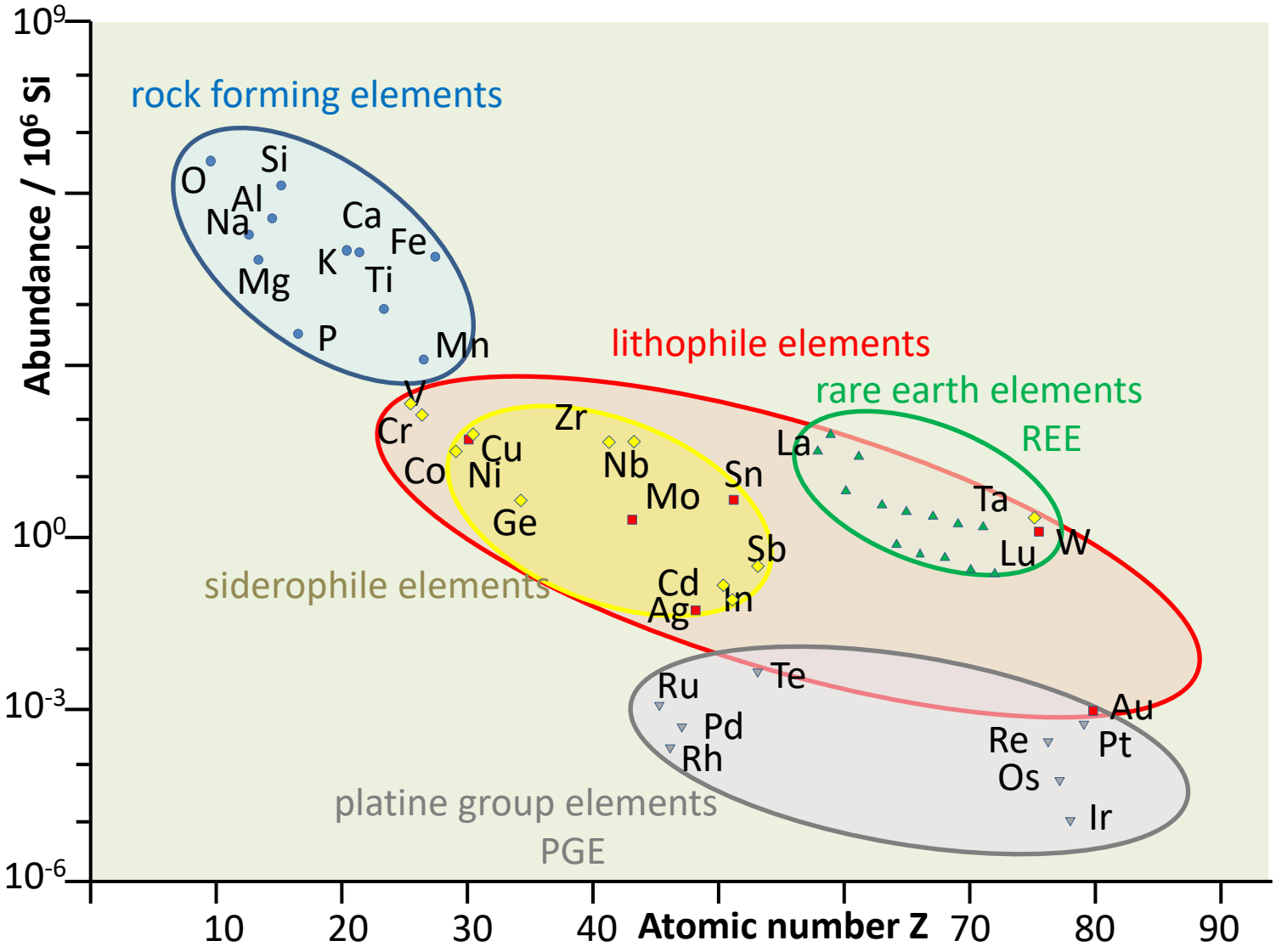

Vigneresse & Truche Fig. 2

melt	metals	MVP
T	Cu, Mo	H_2O CO_2
SiO_2	D	Cl F
η	$K^{me/mvp}$	S

Direct

Inverse

melt	metals	MVP
T	Cu, Mo	H_2O CO_2
SiO_2	D	Cl F
η	$K^{me/mvp}$	S

Iterative

melt	metals	MVP
T	Cu, Mo	H_2O CO_2
SiO_2	D	Cl F
η	$K^{me/mvp}$	S

Vigneresse & Truche

Fig. 3

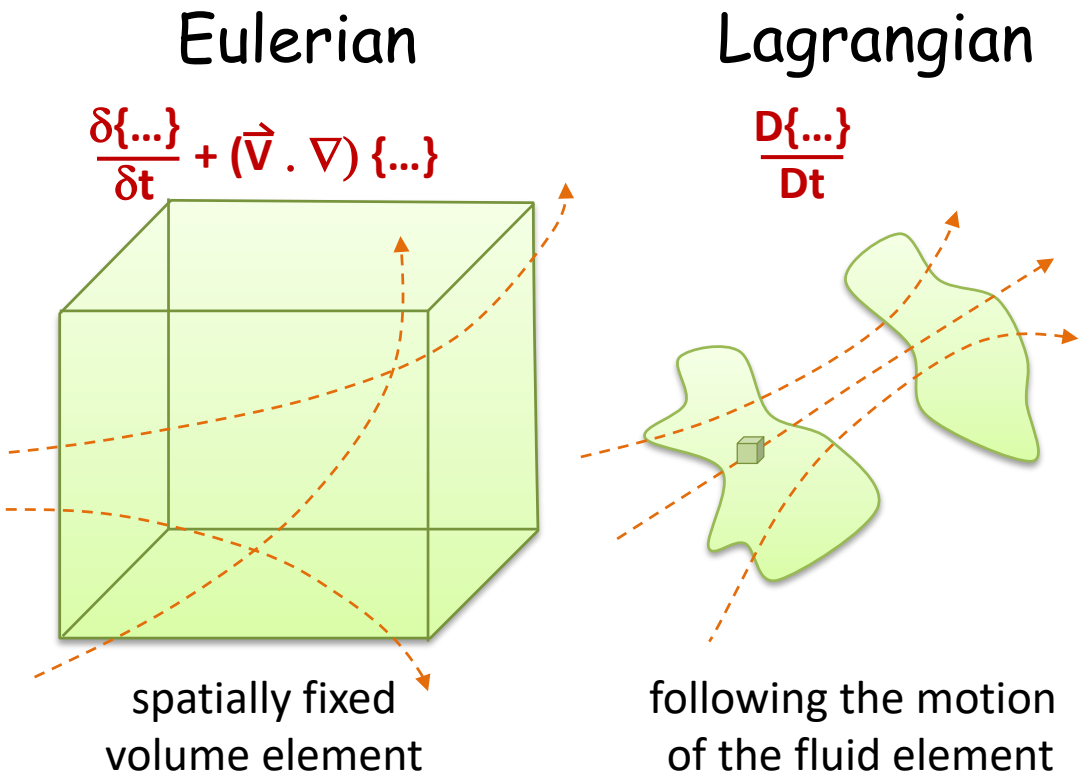

Vigneresse & Truche Fig. 4

Lattice Boltzmann scheme

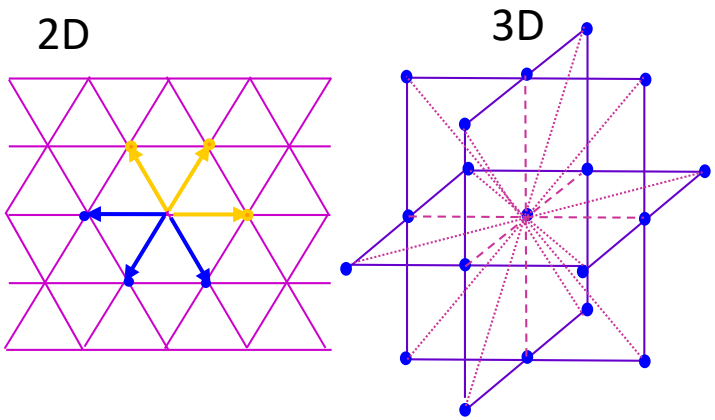

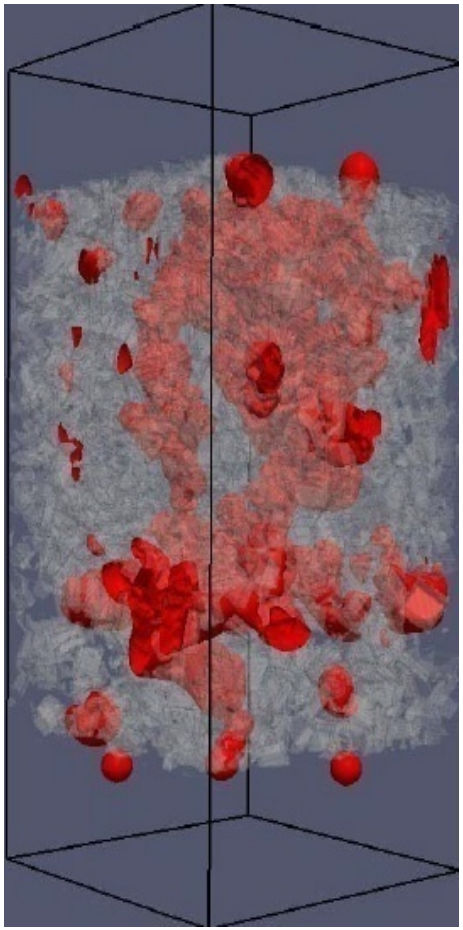

gas flow in a mush
(Xstal 0.55)

Vigneresse & Truche

Fig. 5

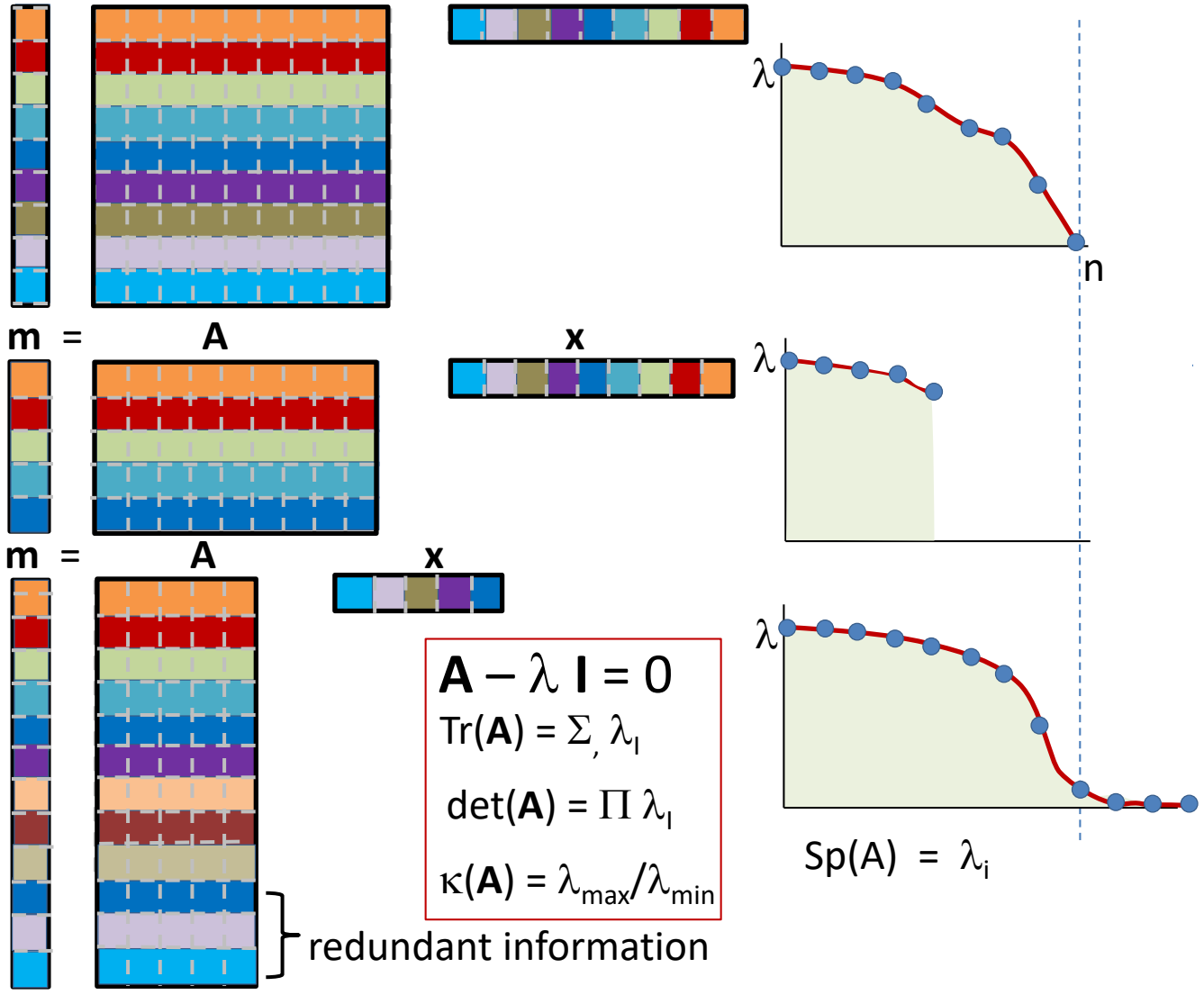

Vigneresse & Truche Fig. 6

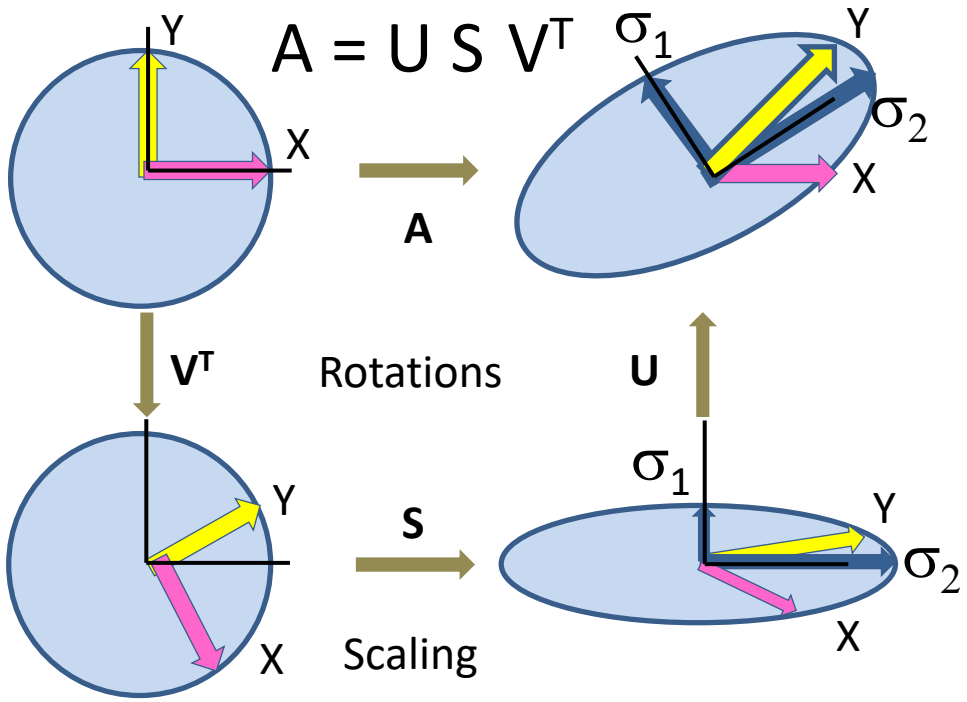

Vigneresse & Truche

Fig. 7

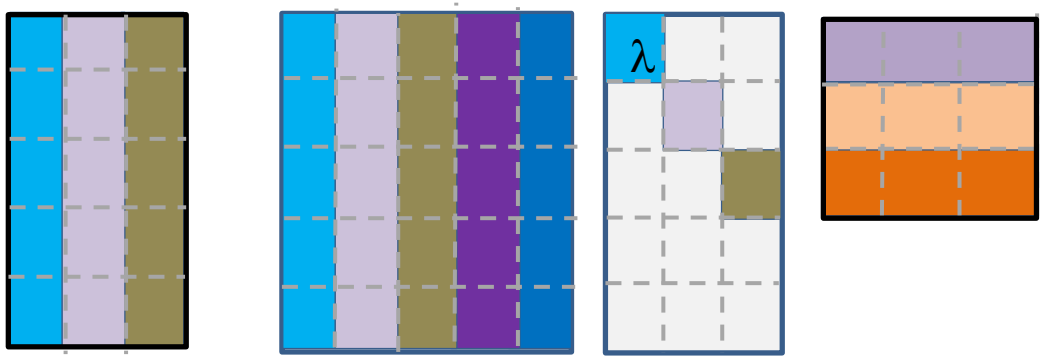

$A_{(m*n)} = U_{(m*m)} * S_{(m*n)} * V^T_{(n*n)}$

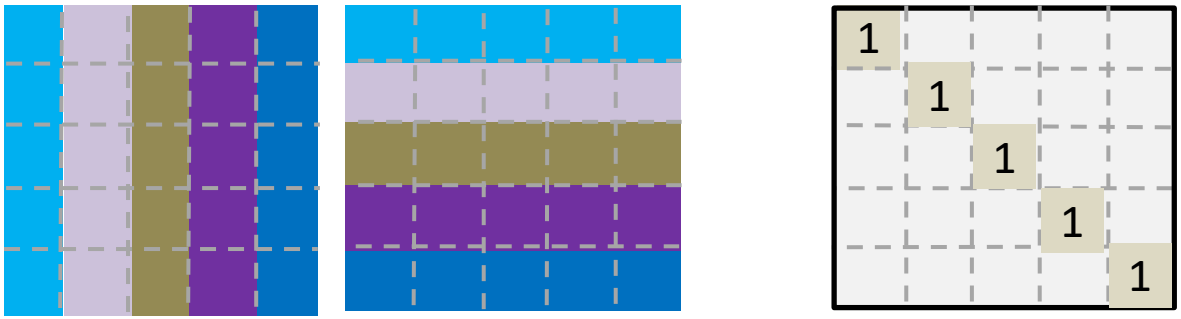

$U * U^T = I$

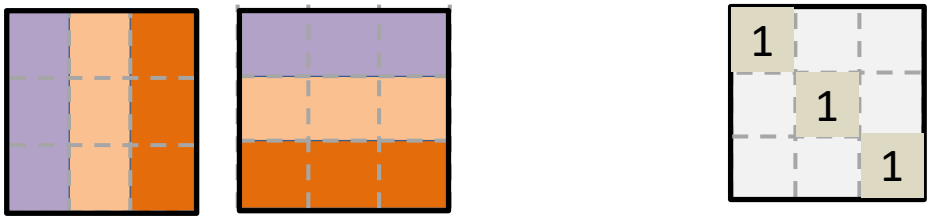

$V * V^T = I$

Vigneresse & Truche Fig. 8

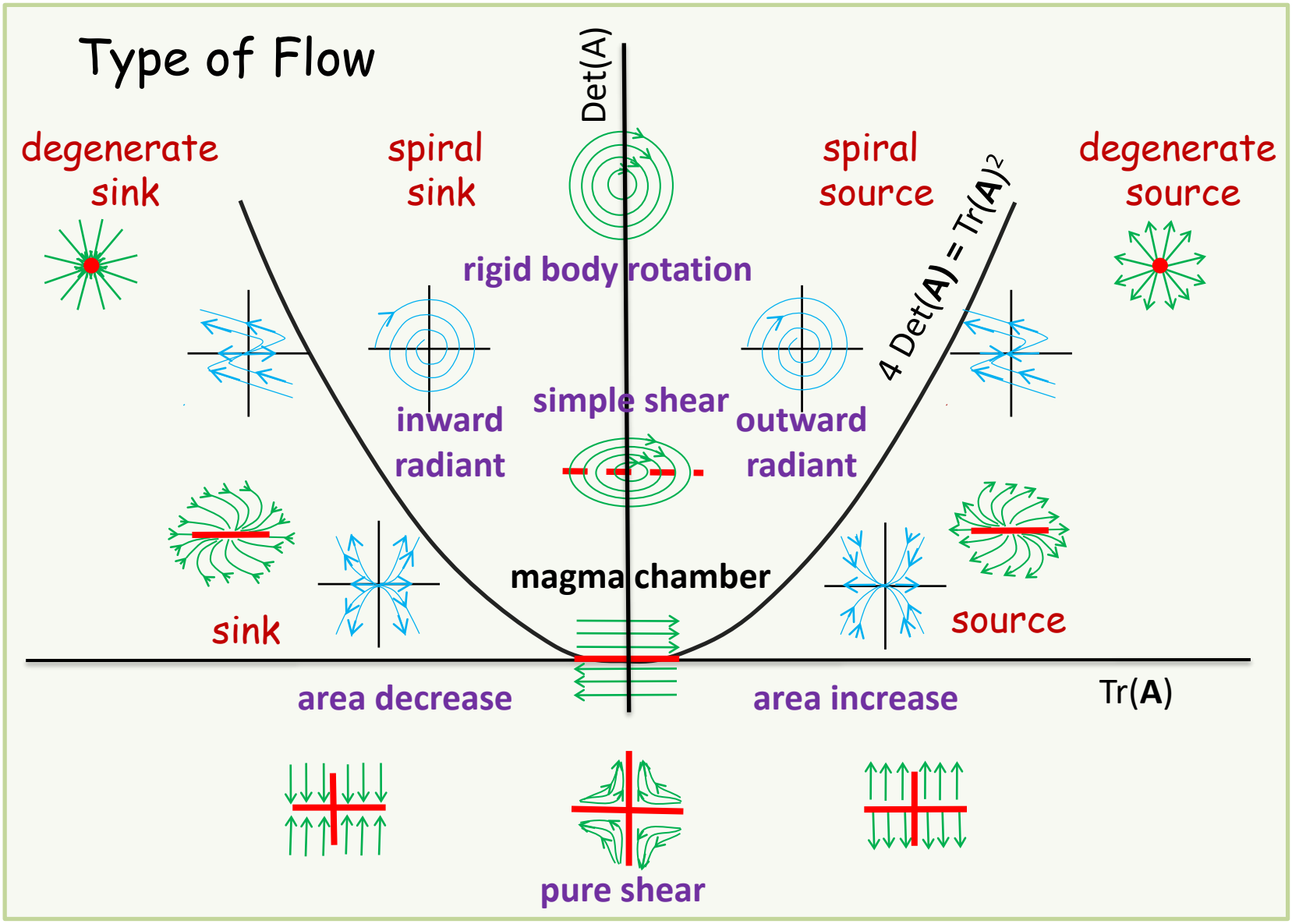

Vigneresse & Truche Fig. 9

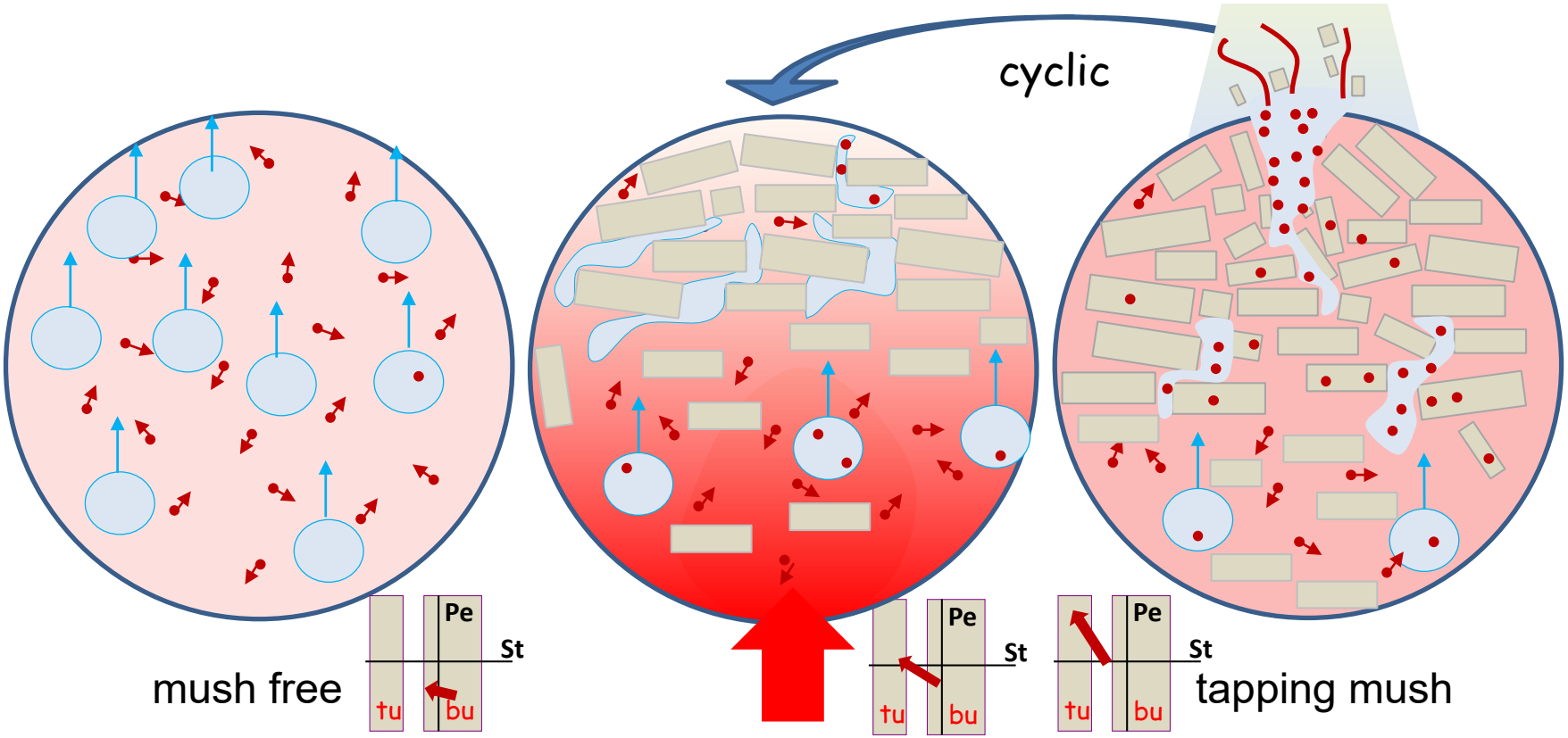

Vigneresse & Truche

Fig. 10

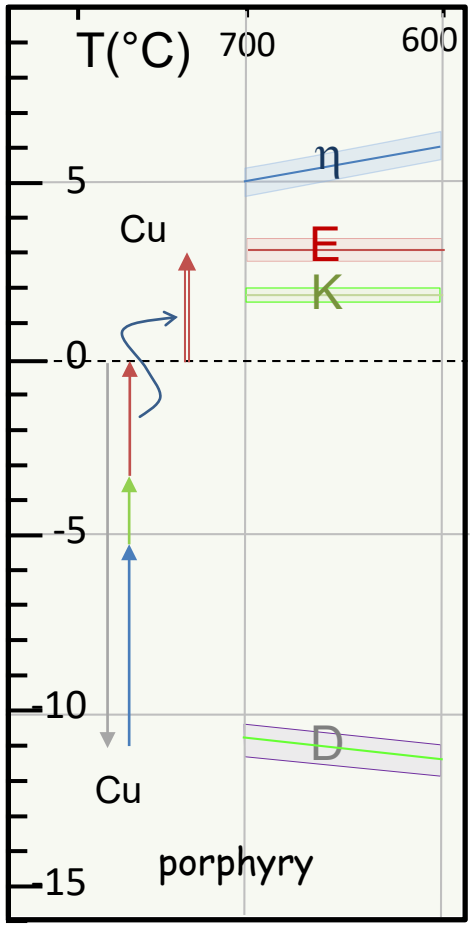

Vigneresse & Truche

Fig. 11